



저작자표시-비영리-변경금지 2.0 대한민국

이용자는 아래의 조건을 따르는 경우에 한하여 자유롭게

- 이 저작물을 복제, 배포, 전송, 전시, 공연 및 방송할 수 있습니다.

다음과 같은 조건을 따라야 합니다:



저작자표시. 귀하는 원저작자를 표시하여야 합니다.



비영리. 귀하는 이 저작물을 영리 목적으로 이용할 수 없습니다.



변경금지. 귀하는 이 저작물을 개작, 변형 또는 가공할 수 없습니다.

- 귀하는, 이 저작물의 재이용이나 배포의 경우, 이 저작물에 적용된 이용허락조건을 명확하게 나타내어야 합니다.
- 저작권자로부터 별도의 허가를 받으면 이러한 조건들은 적용되지 않습니다.

저작권법에 따른 이용자의 권리는 위의 내용에 의하여 영향을 받지 않습니다.

이것은 [이용허락규약\(Legal Code\)](#)을 이해하기 쉽게 요약한 것입니다.

[Disclaimer](#)

공학석사 학위논문

**Effect of Alloying Elements and
Process Parameters on Internal Macro-
segregation Behavior of Aluminum
Alloys Fabricated by Twin-roll Casting**

쌍롤박판주조법 중에 합금원소 첨가 및 공정
변수에 따른 알루미늄 합금 판재 내부 편석 거동
분석

2018 년 12 월

서울대학교 대학원

재료공학부

Tianzhao Wang

Effect of Alloying Elements and Process Parameters on Internal Macro-segregation Behavior of Aluminum Alloys Fabricated by Twin-roll Casting

지도교수 신 광 선

이 논문을 공학석사 학위논문으로 제출함

2018년 12월

서울대학교 대학원

재료공학부

Tianzhao Wang

Tianzhao Wang의 석사 학위논문을 인준함

2018년 12월

위 원 장 _____ 정 인 호

(인) 

부위원장 _____ 신 광 선

(인) 

위 원 _____ 최 인 석

(인) 

ABSTRACT

Effect of Alloying Elements and Process Parameters on Internal Macro-segregation Behavior of Aluminum Alloys Fabricated by Twin-roll Casting

Tianzhao Wang

School of Materials Science and Engineering

The Graduate School

Seoul National University

Since Al has a low density and high specific strength along with sound corrosion resistance, the Al alloys have a great potential of application as structural materials in various industries. However, the high fabrication cost compared to conventional steel materials is the main obstacle for wider application.

Twin roll casting (TRC) is a continuous casting method which allows the fabrication of strips directly from melt which helps to decrease the fabrication cost and increase the productivity. Despite all the advantages, the segregation forms during the TRC process is apparently harmful. Internal macro-segregation which is usually located in the center layer of the TRC strips cannot be completely removed by thermomechanical process after the initial

solidification. Therefore, studies on the formation mechanism of different types of segregation and how to reduce segregation are still necessary.

FEM simulation program DEFORM was used to predicted the solidification behavior during the twin-roll casting of Al alloys. The temperature and liquid fraction distribution of Al alloys with various Mg concentration from 0.5% to 5% were investigated based on the thermodynamic properties calculated using JMatPro program. The effect of casting speed on the temperature and liquid fraction distribution was discussed. Specific points along the thickness direction were selected to track the local strain and liquid fraction during the TRC process. According to the calculated results, freeze range increased and heat transfer coefficient decreased with the increasing Mg concentration which both indicated that more segregation can be expected from high Mg alloys. Furthermore, higher casting speed caused the less contacting time between the roll and melt which delayed the cooling process and resulted in more segregation during the TRC process. Besides, the center layer of the cross-section was calculated to have lower cooling rate and higher deformation while the side layer was confirmed with a higher cooling rate.

As one of the most widely used alloying elements for Al alloys, the effect of Mg element on the macro-segregation behavior of twin-roll cast Al alloys was investigated. From experimental results, larger segregation area was found in samples with high Mg and higher casting speed which matched the simulation results. The types and shapes of internal macro-segregation changed with different casting speed. A vortex-shaped segregation was observed in low-speed samples while a banded structure with channel segregation was found in high-speed samples.

13 different casting parameters were employed to investigate the effect of casting parameters on the internal macro-segregation behavior of commercial AA6016 alloy and the channel segregation free diagram was constructed based on the experimental results.

Keywords: Al-Mg alloys, AA6016 Alloys, Twin-roll Casting, Micro-structure,

Internal Macro-segregation

Student Number: 2016-28172

Contents

1. Introduction	1
1.1 Application of Al Strips	1
1.2 Al Twin-roll Casting.....	2
1.3 Surface and Internal Macro-segregation in Twin-roll Cast Aluminum Strips.....	4
1.4 Current Research Objectives.....	6
Bibliography	8
2. Experimental method	11
2.1 Twin-roll Caster in Current Study.....	11
2.2 Microstructure Observation	11
3. Thermo-dynamic and Finite Element Method simulation of the solidification behavior of TRC aluminum alloys	14
3.1 Introduction.....	14
3.2 Experimental.....	17
3.3 Results and discussions.....	20
3.3.1 Solidification behavior of Al-xMg binary alloys during the TRC process	20
3.3.2 FEM simulation of the solidification behavior during the TRC process with different Mg additions	26

3.3.3 FEM simulation of the solidification behavior during the TRC process of Al-4Mg alloy with different casting speeds	29
3.4 Conclusion	30
Bibliography	35
4. Effect of alloying elements and casting speed on internal macro-segregation of Al-Mg binary alloys during the TRC process	36
4.1 Introduction.....	36
4.2 Experimental.....	37
4.3 Results and discussions.....	41
4.3.1 Effect of alloying elements on the internal macro-segregation of TRC Al-xMg strips	41
4.3.2 Effect of casting speed on the internal macro-segregation of TRC Al-4Mg strips.....	42
4.3.3 Discussion of the formation mechanism of different segregation types and the effect of segregation behavior on final properties in current study.....	57
4.4 Conclusion	61
Bibliography	62
5. Effect of casting parameters on internal macro-segregation of commercial AA6016 alloy.....	64
5.1 Introduction.....	64

5.2 Experimental	65
5.3 Results and discussions.....	67
5.4 Conclusion	72
Bibliography	73
6. Final conclusion	75

List of Tables

Table 2.1 Parameters of the Twin-roll Caster.....	13
Table 2.2 Components of etching reagents.	13
Table 3.1 Chemical compositions of investigated binary Al-Mg alloys. (wt.%).....	18
Table 3. 2 Solidification behavior of Al-xMg binary alloys calculated by JMatPro.....	25
Table 4.1 Chemical compositions of as-TRC binary Al-Mg alloys. (wt.%)	39
Table 4.2 Casting parameters and results of Al-Mg alloys	40
Table 4.3 Casting parameters and results of Al-4Mg alloys	45
Table 5.1 Casting parameters and results of AA6016 alloys	66

List of Figures

Figure 1.1 The difference between TRC process and conventional DC process.....	7
Figure 2.1 Schematic illustration of the twin-roll caster.	12
Figure 3.1 Schematic illustration of solidification procedure during TRC [1].....	15
Figure 3.2 Development of vortex with stagnation points.....	16
Figure 3.3 Two-dimension schematic illustration of TRC simulation using DEFORM.	19
Figure 3.4 Al-Mg phase diagram	21
Figure 3.5 Solidification curves of Al-xMg binary alloys during the TRC process.....	22
Figure 3.6 Elapsed temperature interval/solid fraction curves of Al-xMg binary alloys during the TRC process.....	23
Figure 3.7 The change of thermal conductivity during the solidification of Al-xMg binary alloys	24
Figure 3.8 Temperature distribution of Al-xMg binary alloys during	

the TRC process.....	28
Figure 3.9 Liquid fraction distribution of Al-xMg binary alloys during the TRC process	28
Figure 3.10 Temperature distribution and liquid fraction distribution of Al-4Mg binary alloy during the TRC process under different casting speeds.....	31
Figure 3.11 Liquid fraction at specific points during the TRC process.	32
Figure 3.12 Strain in vertical direction at specific points during the TRC process.....	33
Figure 3.13 Strain in horizontal direction at specific points during the TRC process.....	34
Figure 4.1 Microstructure of longitudinal cross-section of TRC Al-xMg alloys: Al-0.5Mg alloys cast at (a) 3.22mpm and (b) 2.63mpm; Al-1.0Mg alloys cast at (c) 3.22mpm and (d) 2.63mpm; Al-2.0Mg alloys cast at (e) 3.22mpm and (f) 2.63mpm; Al-3.0Mg alloys cast at (g) 3.22mpm and (h) 2.63mpm, Al-4.0Mg alloys cast at (i) 3.22mpm and (j) 2.63mpm Al-5.0Mg alloys cast at (k) 3.22mpm and (l) 2.63mpm.	44

Figure 4.2 Microstructure of as-cast Al-4%Mg strips examined by an optical microscope under polarized light. Longitudinal Cross-section of strips cast at: (a) 2.63mpm, (b) 3.22mpm, (c) 3.96mpm, and (d) 5.28mpm. Banded Structure in strips cast at: (e) 3.96mpm and (f) 5.28mpm.46

Figure 4.3 Mg element distribution in longitudinal cross-section of strips cast at: (a) 3.22mpm and (b) 2.63mpm; The concentration of Mg element changes along thickness direction of strips cast at: (c) and (e) at 3.22mpm and (d) and (f) at 2.63mpm50

Figure 4.4 Micro-structure of segregation region in strips cast at: (a) 3.96mpm, (b) 3.22mpm, and (c) 2.63mpm (under polarized light).....51

Figure 4.5 FEGSEM micrographs and EDAX point scan results of the segregation region in as-TRC samples cast at: (a) 3.22mpm and (b) 2.63mpm52

Figure 4.6 Grain structures of as-cast Al-4%Mg strips examined by an optical microscope under polarized light. Longitudinal cross-section of strips cast at: (a) 2.63mpm, (b) 3.22mpm, (c) 3.96mpm, and (d) 5.28mpm.53

Figure 4.7 Grain structure of as-cast and as-homogenized TRC Al-

4%Mg strips by an optical microscope under polarized light. Longitudinal cross-section of strips cast at: (a) as-TRC cast at 2.63mpm, (b) as-homogenized(30min) strip cast at 2.63mpm, (c) as-homogenized(12h) strip cast at 2.63mpm, (d) as-TRC cast at 3.22mpm, (e) as-homogenized(30min) strip cast at 3.22mpm, (f) as-homogenized(12h) strip cast at 3.22mpm,.....54

Figure 4.8 Strain-stress curves of: (a) as-cast samples, (b) samples homogenized for 30min, and (c) samples homogenized for 12h.55

Figure 4.9 Mechanical properties of as-TRC strips cast at different speeds: (a) shows the relation between strength and casting speed of as-cast strips, (b) shows the relation between strength and casting speed of as-homogenized (30min) strips, (c) shows the relation between strength and casting speed of as-homogenized (12h) strips, (d) shows the relation between modulus of toughness and casing speed of as-cast and as-homogenized strips.56

Figure 5.1 (a) loading weight-thickness curve and (b) casting speed-thickness curve constructed with experimental results...68

Figure 5.2 Microstructure of longitudinal cross-section of as-TRC AA6016 alloy.....70

Figure 5.3 Channel segregation free diagram of AA6016 alloy
during the TRC process.71

1. Introduction

1.1 Application of Al Strips

Aluminum as a structural material has been widely used in various industries. In particular, Aluminum strips used as vehicle body can reduce the total weight of vehicles which helps the reduction of carbon di-oxide emission from automobiles. Especially in Europe, aluminum takes place around 80% of the produced cars while the proportion was about 2% 20 years ago [1]. The huge increase of aluminum application of automotive industries can be explained by the increasing demand for fuel economy and carbon di-oxide emission reduction. As an economical alternative material to steel, aluminum does have several advantages, however, high fabrication and assembly cost were considered as the key obstacles [2].

Apparently, as one of the most widely used light metals, aluminum has big advantages over steel. Firstly, aluminum has a density of 2.7 g/cm^3 which is almost 33% of steel which is much more dense with a density of 8.0 g/cm^3 [3]. The total mass decrease brought by the use of aluminum instead of steel may be up to 120kg for each car which indicates a 982 million-liters reduction in fuel and a 2.3 million-tons reduction in CO_2 emission [4]. Despite the light weight, Al is more malleable and elastic than steel which allows more complicated deform process and help to expand the dimensional limitation of manufacture. Furthermore, Al is naturally corrosion resistant without any surface treatment [5].

However, the price of aluminum is about five times more expensive than steel due to the high primary price and complicated fabrication process [2,5]. The price of Al

is continually fluctuating based on the global supply and demand which is generally more expensive than stainless steel. The cost of raw materials has a direct impact on the price of the finished products [2]. Therefore, more studies should be carried out on fabrication process with higher efficiency and lower cost.

1.2 Al Twin-roll Casting

As mentioned in last paragraph, the demand for vehicles with the light structural body has increased in recent decades as an alternative material for mild steel in automobile industries, however, the use of aluminum in automobile industries are facing challenges: higher cost than steel, and difficulties in large-scale production. Twin-roll casting (TRC) which has been used for 60 years for aluminum strips fabrication and has been considered as a casting process which can be used to reduce the production cost since strips can be obtained directly from the molten alloy through the twin-roll casting process [6,7], see Fig. 1.1. TRC offers several advantages including less capital investment, lower energy consumption, and limited space [6,8]. Besides, refined grain structure and improved solid solubility can be expected from TRC strips due to the rapid cooling during the TRC process [9,10].

Despite advantages given above, casting speed of the TRC process limits the productivity which has been considered as a main issue for strips casting of aluminum [2,6,7,8]. Various TRC processes were applied to remain the competitive compared with other fabrication processes. Generally, TRC processes can be divided into vertical TRC, conventional horizontal TRC, and inclined TRC [6,11,12,13]. Conventional horizontal TRC with a pair of

horizontal assembled rolls is usually employed for further downstream rolling process at a relatively low casting speed [6]. However, limited casting speed causes lower productivity which is not applicable for mass production. Furthermore, in terms of aluminum TRC, the frequent sticking occurs during the TRC process between strips and rolls can cause severe problems. Besides, a larger proportion was confirmed to be columnar structure in the conventional TRC aluminum strips with equiaxed grains in the mid-layer of thickness direction. Better mechanical properties can be expected with more equiaxed grains across the thickness direction which can be obtained with higher cooling rate or lower casting temperature. When the casting is carried out with a low melt temperature, unwanted early solidification of melt inside the nozzle occurs frequently [11]. In addition, only limited alloy compositions are castable. Especially, casting of highly alloyed systems are still limited due to its larger solidification range.

A vertical TRC was introduced by T. Haga to solve those problems with much higher casting speed and less sticking problems [11,12]. By using a vertical TRC, aluminum strips can be cast at a high speed up to 180mpm with a pair of copper rolls without any lubricant coatings [11]. A larger area of equiaxed grain structure was observed in vertical TRC strips which offers better mechanical properties [12]. However, TRC process was commonly followed by rolling process to get final products [6]. With employment of a vertical TRC, various difficulties may also be taken into consideration for mass production.

Taking both the features of conventional and vertical into account, an inclined TRC was employed with a cooling slope to achieve semi-solid condition during filling stage of TRC process. A semisolid slurry with a solid fraction of about 5-10% was formed with a cooling slope and then transferred to a pair of inclined rolls. Casting speed was increased to 90mpm and also offer the possibilities of further rolling processes [13].

1.3 Surface and Internal Macro-segregation in Twin-roll Cast Aluminum Strips

Both surface and internal segregations can form during the TRC process [6]. Bleeds, dents, and cracks may arise on the surface under certain casting conditions [14,15]. Meanwhile, center-line segregation which is considered the most harmful internal segregation may also form during the TRC process [7]. The formation of surface segregates was investigated to be a transportation of the enrichment of alloying elements at inter-dendrite/grain towards surface. This transportation occurs when the contact between materials and rolls are weak induced by the fluctuation of the contact between loaded melt and rolls [15]. Surface defects trend to form when the tiny buckles occur on surface and refilling of the buckled empty surfaces, and surface defects free diagram was reported in Ch. Gras's work [14].

Compare to surface segregation, internal segregation has been considered as the most harmful defect in TRC strips. In particular, a solution enriched central zone can form through the thickness direction which is usually called

normal segregation. Eutectic forming elements (such as Mg, Fe, Si, Ni, and Zn) trend to form positive enrich region while peritectic forming elements (such as Ti, Cr, and V) trend to form solution poor depleted region [16]. During TRC process, since the cooling rate is usually at a high level, normal segregations barely form in a TRC structure. Commonly, center-line segregation, deformation segregation, and banded structure were reported in TRC aluminum strips under specific conditions [7,17,18].

Various attempts have also been carried out to avoid, or at least to reduce the internal segregation. As mentioned above, a vertical twin-roll caster was used to fabricate Al strips with different melt loading methods, both casting speed and mechanical properties were improved by a semi-solid melt loading [11,12]. A twin-roll casting under ultrasonic energy field was reported to have a grain refinement effect along with a reduction of precipitated phases which can help to reduce the center-line segregation. The tensile strength and yield strength increased by 5.8% and 13% using this novel process [19]. Melt preconditioning by intensive shear was used before casting and a reduced center-line segregation with uniform micro-structure across thickness direction [8,20]. A twin-roll casting combined with static magnetic field and pulse electric current field was studied and both fields were proved to be effective in controlling defects during the TRC process [21].

1.4 Current Research Objectives

As a casting process with the potential application in various industries, TRC has both merits and demerits. Realization of mass production of aluminum strips by TRC with sound properties will help to reduce the environmental pollution induced by automobile emission. Internal macro-segregation has been widely considered as the most harmful defects in TRC strips. Many studies focusing on the formation and reduction of internal macro-segregation were carried out by researchers around the world, however, still there are unclear mechanisms of internal macro-segregation during TRC which need further study and explanation. The main research objectives of this thesis are as follows:

1. Analyzing the effect of the alloying elements and the TRC process parameters on solidification behavior of aluminum alloys based on thermodynamic calculations and FEM predictions.
2. Fabrications of aluminum alloys with different alloying elements under various TRC parameters.
3. The effect of the alloying element and the TRC process parameters on internal macro-segregation behavior of aluminum alloys.
4. Optimization of TRC process of commercial AA6016 alloy.

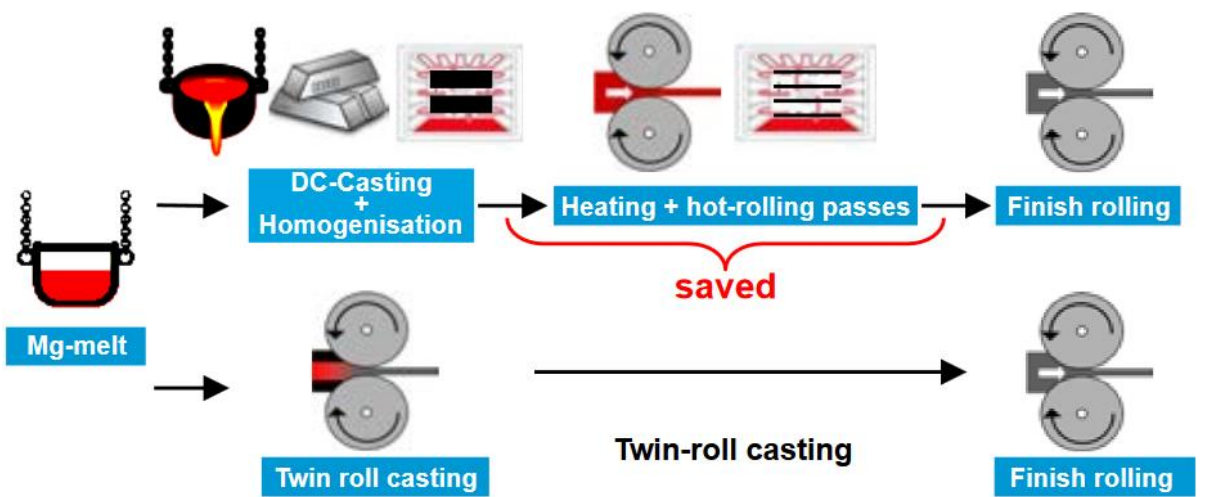


Figure 1.1 The difference between TRC process and conventional DC process.

Bibliography

- [1] I.N. Fridlyander, V.G. Sister, O.E. Grushko, V.V. Berstenev, L.M. Sheveleva, L.A. Ivanova, "Aluminum Alloys: Promising Materials in the Automotive Industry, Metal Science and Heat Treatment", 44(2002) 365-370.
- [2] A. Kelkar, R. Roth, J. Clark, "Automobile Bodies: Can Aluminum be an Economical Alternative to Steel?", JOM, 53(2001) 28-32,
- [3] M. Austin, "Materials Competition in the Automotive Industry", Steel Times, 225(1997), 141-146.
- [4] A.L. Taub, "Reducing Weight for Transportation Applications: Technology Challenges and Opportunities", Magnesium Technology 2015, 2015, 3.
- [5] K.R. Brown, M.S. Venie, R.A. Woods, "The Increasing Use of Aluminum in Automotive Applications-JOM", 47(1995), 20-23.
- [6] R. Cook, P.G. Grocock, P.M. Thomas, D.V. Edmonds, J.D. Hunt, "Development of the twin-roll casting process", Journal of Materials Processing Technology, 1995, pp.76-84.
- [7] M. Yun, S. Lokyer, J.D. Hunt, "Twin roll casting of aluminum alloys", MSE A, 2000, pp.116-123.
- [8] N.S. Barekar, B.K. Dhindaw, "Twin-roll Casting of Aluminum Alloys- An overview, Materials and Manufacturing Processes", 29(2014), 651-661.
- [9] S.J. Park, H.C. Jung, K.S. Shin, "Deformation Behaviors of Twin Roll Cast Mg-Zn-Ca Alloys for Enhanced Room-temperature Formability", Materials Science and Engineering: A, 679(2017), 329-339.

- [10] S.J. Park, H.C. Jung, K.S. Shin, "Analysis of the Solidification and Deformation Behaviors of Twin Roll Cast Mg-6Al-X Alloys", *Metals and Materials International*, 22(2016), 1055-1064.
- [11] T. Haga, K. Takahashi, M. Ikawa, H. Watari, "A vertical-type Twin Roll Caster for Aluminum Alloy Strips", *Journal of Materials Processing Technology*, 140(2003), 610-615.
- [12] T. Haga, K. Takahashi, M. Ikawa and, H. Watari, "Twin Roll Casting of Aluminum Alloy Strips, *Journal of Materials Processing Technology*", 153(2004), 42-47.
- [13] T. Haga, "Semisolid Strip Casting Using a Twin Roll Caster Equipped with A Cooling Slope", *Journal of Materials Processing Technology*, 130(2002), 558-561.
- [14] C. Gras, M. Meredith, J.D. Hunt, "Microdefects Formation during The Twin-roll Casting of Al-Mg-Mn Aluminum Alloys", *Journal of Materials Processing Technology*, 167(2005), 62-72.
- [15] B. Forbord, B. Andersson, F. Ingvaldsen, O. Austevik, J.A. Horst, I. Skauvik, "The Formation of Surface Segregates during Twin Roll Casting of Aluminum Alloys", 415(2006), 12-20.
- [16] A. Unal, "Continuous Casting of Aluminum", U.S. Patent 6,672,368, issued January 6, 2004.
- [17] M.S. Kim, S. Kumai, "Solidification Structure and Casting Defects in High-speed Twin-roll Cast Al-2 mass% Si Alloy Strip", *Materials Transactions*, 54(2013), 1930-1937.
- [18] M.S. Kim, S.H. Kim, H.W. Kim," Deformation-induced Center Segregation in

Twin-roll Cast High-Mg Al-Mg Strips”, *Scripta Materialia*, 152(2018), 69-73

[19] C. Shi, K. Shen, “Twin-roll Casting 8011 Aluminum Alloy Strips under Ultrasonic Energy Field”, *International Journal of Lightweight Materials and Manufacture*, 1(2018), 108-114.

[20] K.H. Kim,” The Effect of Melt Conditioning on Segregation of Solute Elements and Nucleation of Aluminum Grains in a Twin Roll Cast Aluminum Alloy”, *Metallurgical and Materials Transactions A*, 45(2014), 4538-4548.

[21] K.M. Sun, L. Li, S.D. Chen, G.M. Xu, G. Chen, R.D.K. Misra, G. Zhang, “A New Approach to Control Centerline Macrosegregation in Al-Mg-Si Alloys during Twin Roll Continuous Casting”, *Materials Letters*, 190(2017), 205-208.

2. Experimental method

2.1 Twin-roll Caster in Current Study

A conventional horizontal twin-roll caster (see Fig.2.1) with a constant roll gap of 1.5mm was used in this research. A pair of copper rolls with cooling system equipped inside were employed for TRC process in this study. Details about the twin-roll caster were shown in Table 2.1. The diameter of the roll is 140mm. Available casting speeds range from 0~10mpm, while strips are castable with casting speeds from 2.5 to 5.3mpm. Coolant flow rates of the equipped running water tunnels can be adjusted from 0 to 4 gallon/min. A nozzle made by rubiel bulk which resists 1400°C was employed during the TRC casting to offer stable melt flow and feeding. For each single TRC lab-scale casting, up to 3.2 Kg aluminum ingots can be melted inside the hot chamber. During the TRC process, a motor-driven pendulum will move down at a constant speed pushing the melted aluminum into the runner and finally transfer the melt into the rap between two rotating rolls.

2.2 Microstructure Observation

Longitudinal cross-section was taken from the middle part of as-cast strips and mounted with a resin holder to avoid rounding during the mechanical polishing. Samples were carefully polished with SiC suspension followed by electro-polishing with a solution including 30% perchloric acid and 70%

methanol under 15 volts for 10s. For dendrite observation, the Weck's reagent was used to reveal the segregation region and also show the dendrite structure clearly. For grain structure observation, the Barker's reagent was employed to reveal the grain boundaries. Since segregation should also be observed along with grain structure, the Keller's reagent was used to remove the segregation region prior to the anodization with Barker's reagent. Samples were anodized under 15 volts for 150s to get clear images under polarized light. Components of etching reagents used in this study were presented in Table 2.2.

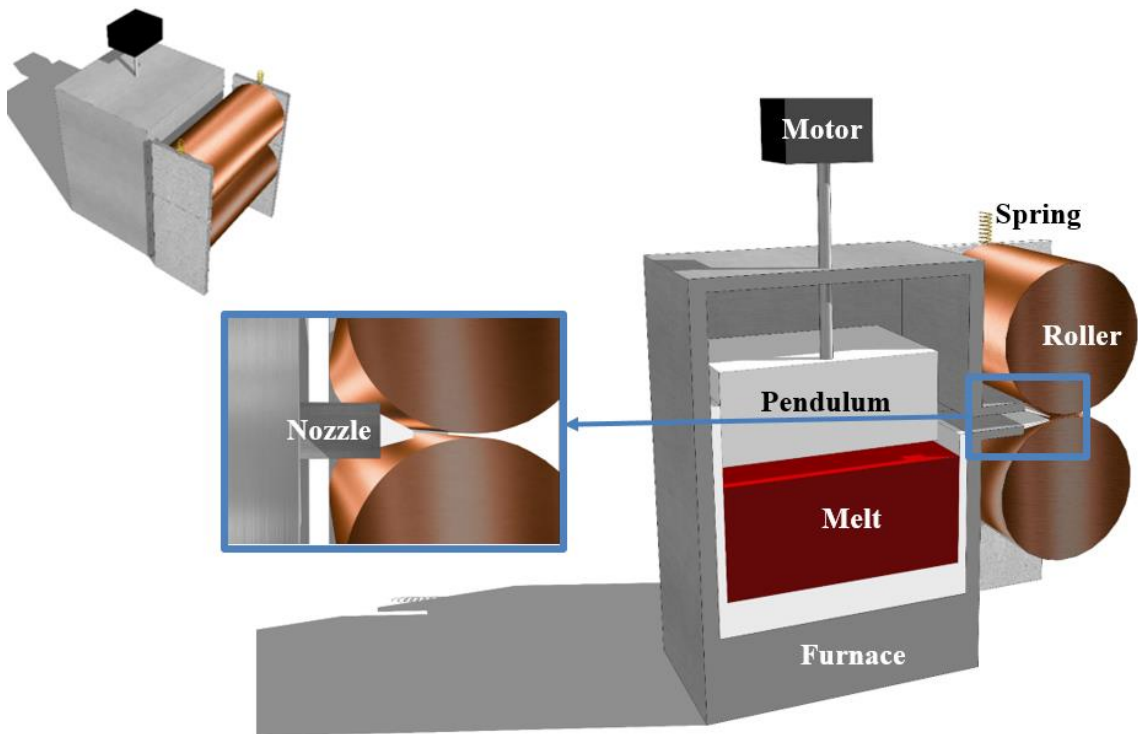


Figure 2.1 Schematic illustration of the twin-roll caster.

Table 2.1 Parameters of the Twin-roll Caster

Roll			
Material	Cu-Be Alloy	Diameter	140mm
Speed Range	0~10 mpm	Coolant Flow Rates	0~4 gallon/min
Nozzle			
Material	Rubiel Bulk	Thickness	3.5mm
Hot-chamber			
Capacity	3.2 kg Al	Max. Temperature	900°C
Pendulum			
Material	Rubiel Bulk	Volume	90*90*180 (mm)

Table 2.2 Components of etching reagents.

Etching Reagents	Solution Components
Keller's	2ml Hydrofluoric acid in 100ml H ₂ O
Weck's	1g NaOH and 4g KMnO ₄ in 100ml H ₂ O
Barker's	1.8% Fluoboric acid in H ₂ O

3. Thermo-dynamic and Finite Element Method

simulation of the solidification behavior of TRC

aluminum alloys

3.1 Introduction

The whole Twin-roll Casting can be considered as a combination of casting and hot-rolling. The whole solidification procedure of the TRC is shown in Fig. 3.1 [1]. Setback is the distance from nozzle to nip-point consists of the sump and the deformation region which is also called as the melt to nip-point distance [2]. The distance required to solidify from the exiting point of nozzle is the sump depth, while the distance between solidus interface and the nip-point of the rolls is the melt to nip-point distance or the deformation region.

Since the microstructure, quality, and defect are all highly influenced by the solidification behavior during the TRC process, various numerical studies had been done by different researchers. J.J. Park numerically analyzed the solidification behavior of a vertical TRC using the rigid-thermoviscoplastic finite-element method to clarify the complex phenomena including melt flow, heat transfer, solidification, and plastic deformation in a vertical TRC [3]. Moreover, he carried out coupled analyses of flow and heat transfer during a horizontal TRC with a commercial AA3003 alloy. In his study, melt flow,

solidification, roll pressure, roll separating force (RSF) were predicted under different casting conditions and the melt was observed to be confined in rotational motions of two vortexes developed during the filling stage [4], see Fig. 3.2. Differential Scanning Calorimetry was employed to analyze the solidification curves with different cooling rate, and the impact of solidification behavior on the occurrence of internal macro-segregation was also investigated with four commercial alloys [5].

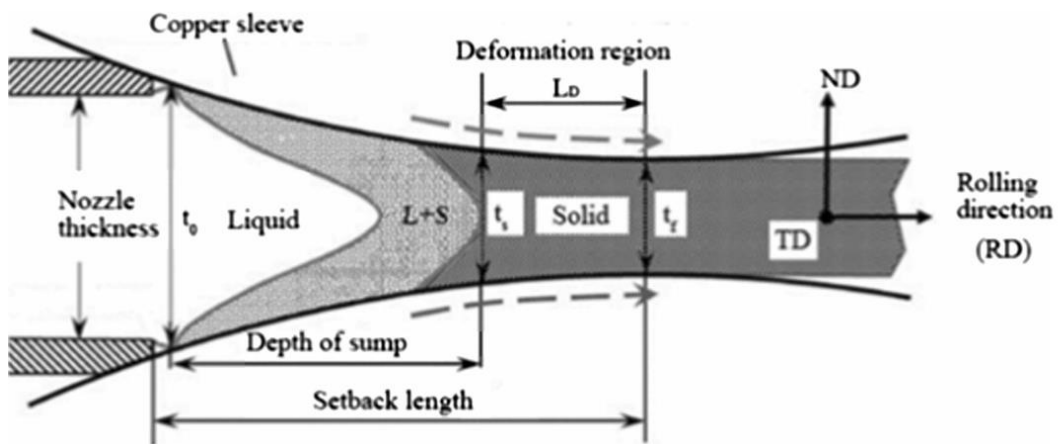


Figure 3.1 Schematic illustration of solidification procedure during TRC [1].

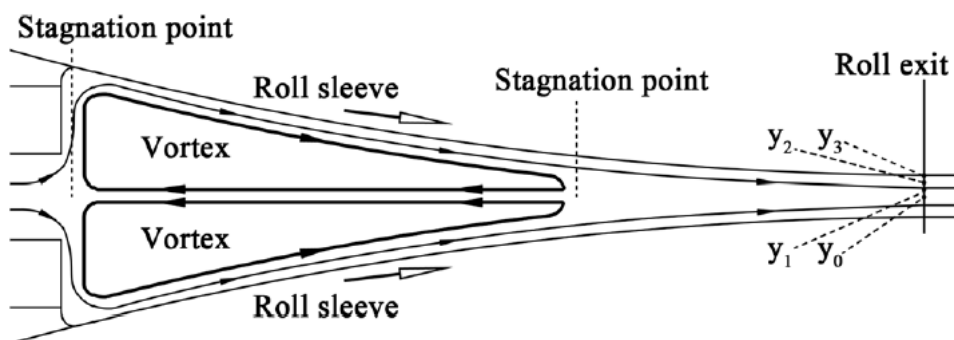


Figure 3.2 Development of vortex with stagnation points.

3.2 Experimental

Solidification behavior of TRC Al binary alloys with nominal compositions in Al-xMg (x=0.5, 1.0, 2.0, 3.0, 4.0, and 5.0 in wt.%) were investigated with a commercial FEM code DFORM software. Chemical compositions of investigated alloys were shown in Table 3.1. For simulation input, specific heat, thermal conductivity, latent heat, and liquid fraction at different degrees were calculate by JMatPro software under the scheil condition.

Flow stress of liquid phase was calculated by following equation from database of flow stress in DEFORM for aluminum alloys:

$$\dot{\epsilon} = A[\sinh(\alpha\bar{\sigma})]^n e^{-\Delta H/RTabs}$$

Where A is a constant, n is strain rate exponent, ΔH is the activity energy, R is gas constant, α is the flow stress, and $\dot{\epsilon}$ is the effective strain rate.

Two-dimension schematic illustration of TRC process in DEFORM software was given in Fig.3.3. Specific points with a constant distance between each other through the thickness direction were tracked during TRC simulation (see Fig.3.3). Thermal-dynamic properties obtained from JMatPro were used for simulation condition definition and the melt temperature was set to 700°C. Finally, appropriate experimental roll rotation speeds were selected for simulation.

Table 3.1 Chemical compositions of investigated binary Al-Mg alloys. (wt.%)

Alloys	Chemical Compositions (wt.%)			
	Mg	Si	Fe	Al
Al-0.5Mg	0.5	-	-	Bal.
Al-1.0Mg	1.0	-	-	Bal.
Al-2.0Mg	2.0	-	-	Bal.
Al-3.0Mg	3.0	-	-	Bal.
Al-4.0Mg	4.0	-	-	Bal.
Al-5.0Mg	5.0	-	-	Bal.

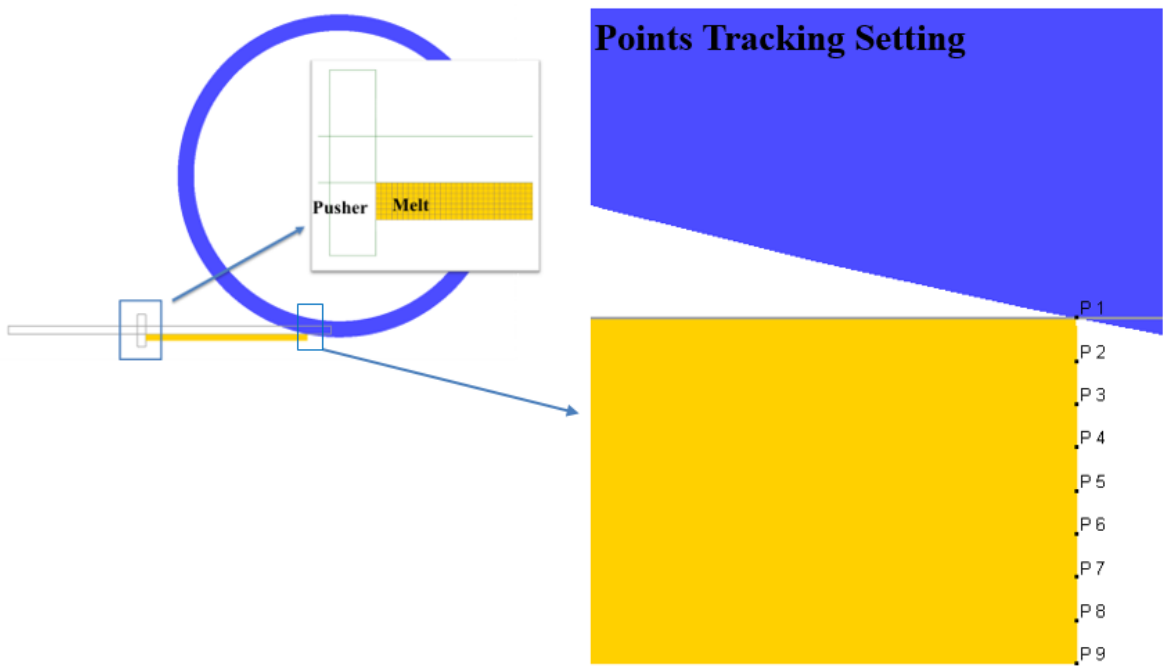


Figure 3.3 Two-dimension schematic illustration of TRC simulation using DEFORM.

3.3 Results and discussions

3.3.1 Solidification behavior of Al-xMg binary alloys during the TRC process

The TRC simulations of Al-xMg binary alloys were carried out to predict the solidification behavior. Fig. 3.4 shows the Mg-Al phase diagram. The solidus temperature, liquidus temperature, and the freeze range were calculated using JMatPro under the Scheil condition with a cooling rate of 250 °C/s which has been reported in recent studies [4,5] and the results were shown in Table 3.2. A decrease of both liquidus temperature and solidus temperature along with an increase of freeze range was confirmed with more addition of Mg.

The solidification curve was presented in Fig. 3.5 showing change in solid fraction with temperatures. With the increasing Mg concentration, both liquidus temperature and solidus temperature decreased and resulted in a larger interval indicating larger freeze range. Fig. 3.6 shows the elapsed temperature interval/solid fraction curves, high Mg addition expanded the solidification interval and promote macro-segregation. Furthermore, the heat transfer between the rolls and melt is one of the key affecting parameters of segregation behavior. Fig. 3.7 shows the change of thermal conductivity of Al-xMg binary alloys during the TRC process, Al-0.5Mg has the highest thermal conductivity during the solidification process indicating better heat transfer between the rolls and the melt which can assist to get higher cooling rate and less segregating possibility. On the other hand, Al-5.0Mg has the lowest

thermal conductivity which delays the heat transfer and trends to segregate in the center-layer.

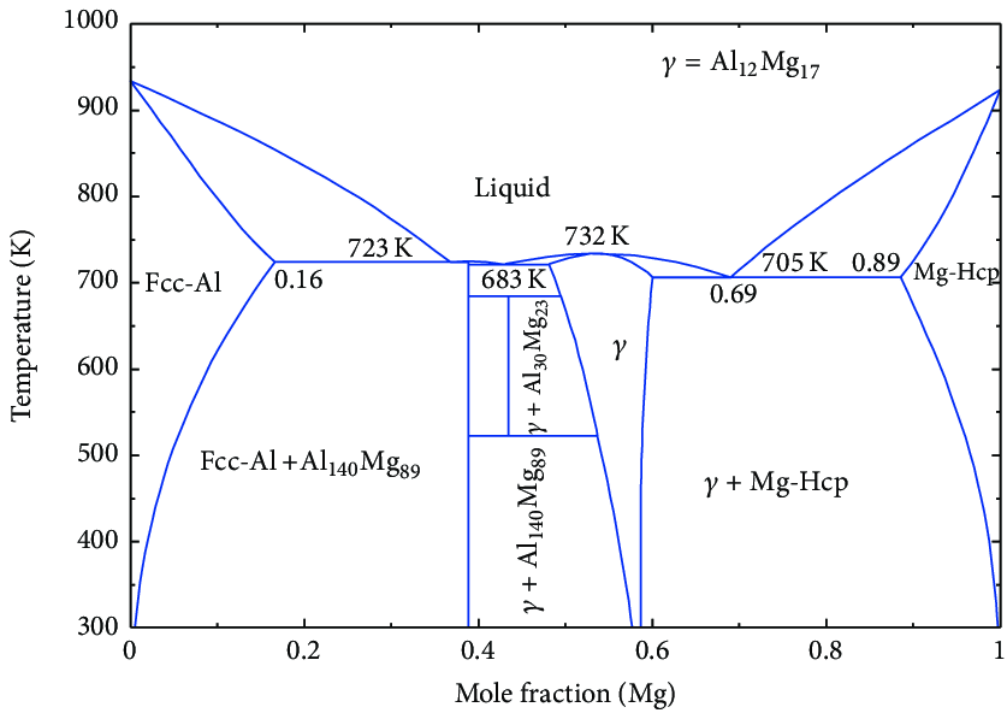


Figure 3.4 Al-Mg phase diagram

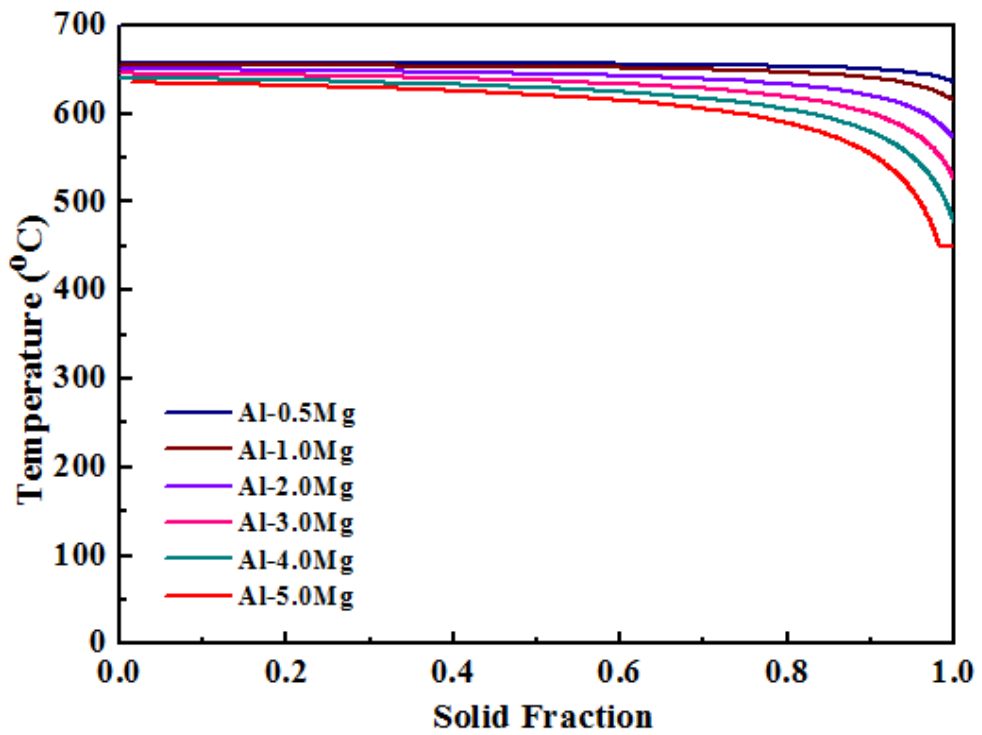


Figure 3.5 Solidification curves of Al-xMg binary alloys during the TRC process

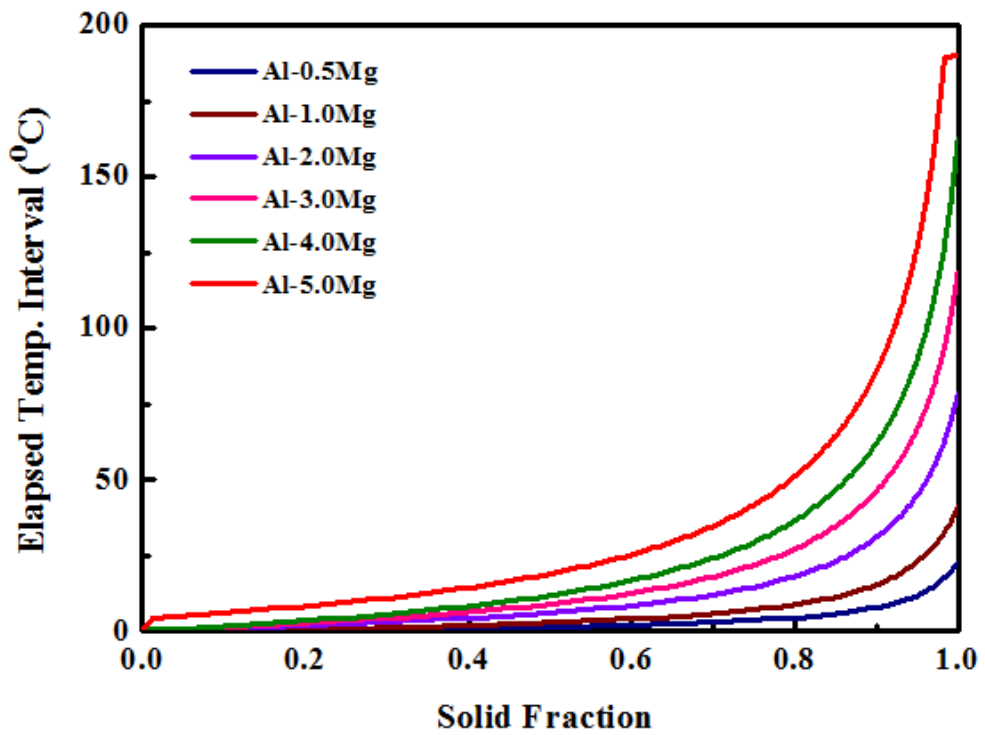


Figure 3.6 Elapsed temperature interval/solid fraction curves of Al-xMg binary alloys during the TRC process

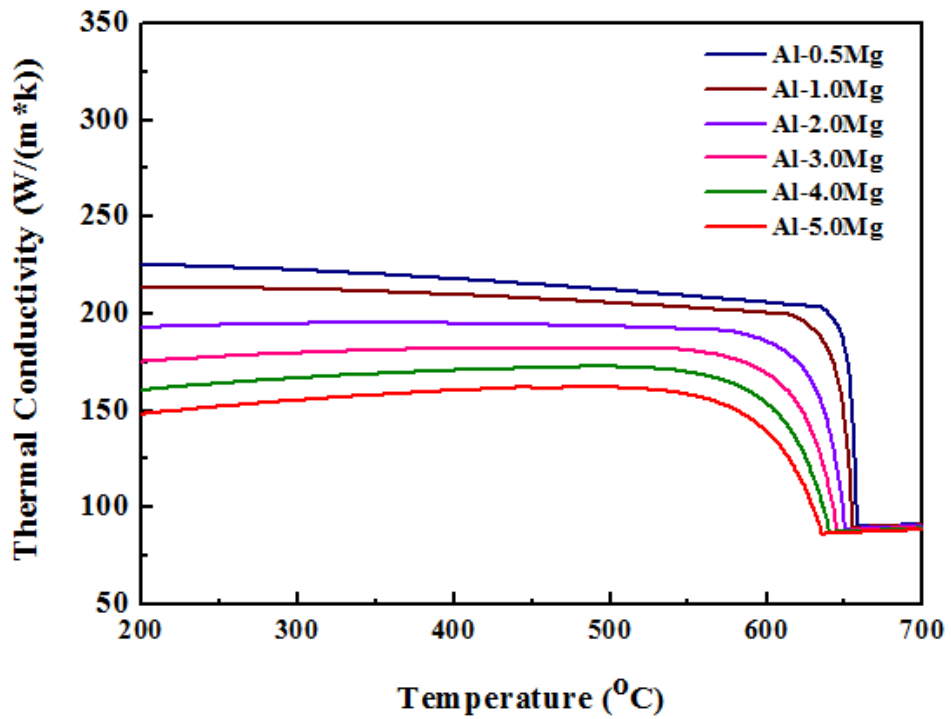


Figure 3.7 The change of thermal conductivity during the solidification of Al-xMg binary alloys

Table 3.2 Solidification behavior of Al-xMg binary alloys calculated by JMatPro.

Alloys	Liquidus Temp. (°C)	Solidus Temp. (°C)	Freeze Range (°C)
Al-0.5Mg	658.0	635.5	22.5
Al-1.0Mg	655.5	614.5	41.0
Al-2.0Mg	651.0	572.5	78.5
Al-3.0Mg	646.0	527.5	118.5
Al-4.0Mg	641.0	478.0	163.0
Al-5.0Mg	636.0	450.0	186.0

3.3.2 FEM simulation of the solidification behavior during the TRC process with different Mg additions

The casting speed was set to 3.22 mpm. The temperature distributions of Al-xMg alloys during the TRC were presented in Fig. 3.8. Side layer of the melt showed a lower temperature due to the higher cooling rate at the fringe while higher temperature was detected at the same position with higher Mg addition which can be explained by the larger freeze range. Fig. 3.9 shows the liquid fraction distribution of Al-xMg binary alloys during the TRC process. Deformation range, i.e., the melt to nip-point distance was calculated from the simulation results. The deformation region which are highly related to the segregation occurrence, is 24.3mm, 21.0mm, 13.4mm, 12.1mm, and 11.8mm for Al-xMg alloys, respectively. With less addition of Mg, larger deformation region was calculated which indicates less tendency of segregation. The Al-5Mg alloy has the longest depth of sump due to its longest freeze range and the lowest thermal conductivity among all the alloys, which may increase the size of the mushy zone and trend to form more macro-segregation like channel segregation and inverse segregation.

Compared to calculated solidification behaviors by JMatPro. When more Mg was added, lower heat transfer coefficient between the rolls and melt induced by the lower thermal conductivity and slower solidification caused by the large freeze range allow more remaining Mg-rich melt near to the end of the solidification reaction which finally formed Mg-rich segregation in the center later of TRC strips. Not only the internal macro-segregation but also

surface quality can be affected by the solidification behavior, and finally the mechanical properties of final product can be influenced by the solidification behavior.

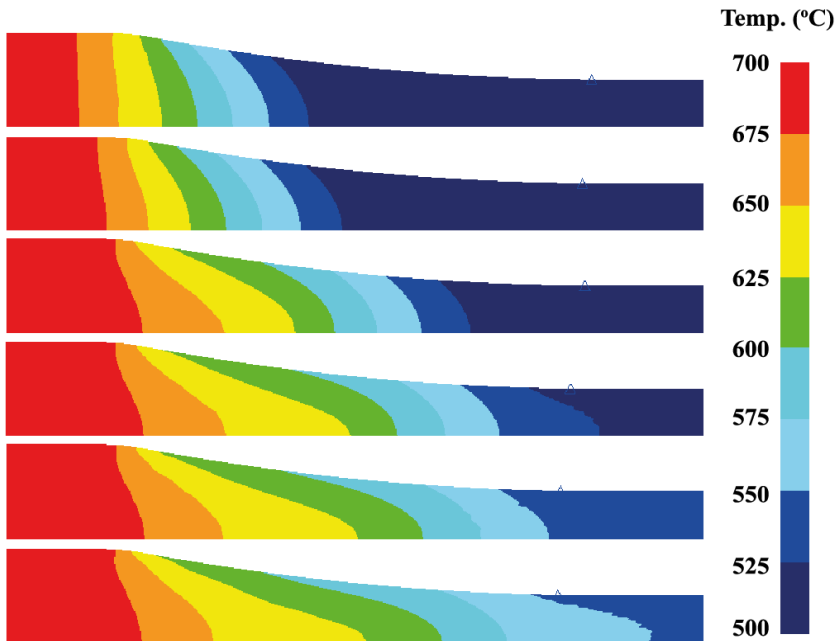


Figure 3.8 Temperature distribution of Al-xMg binary alloys during the TRC process.

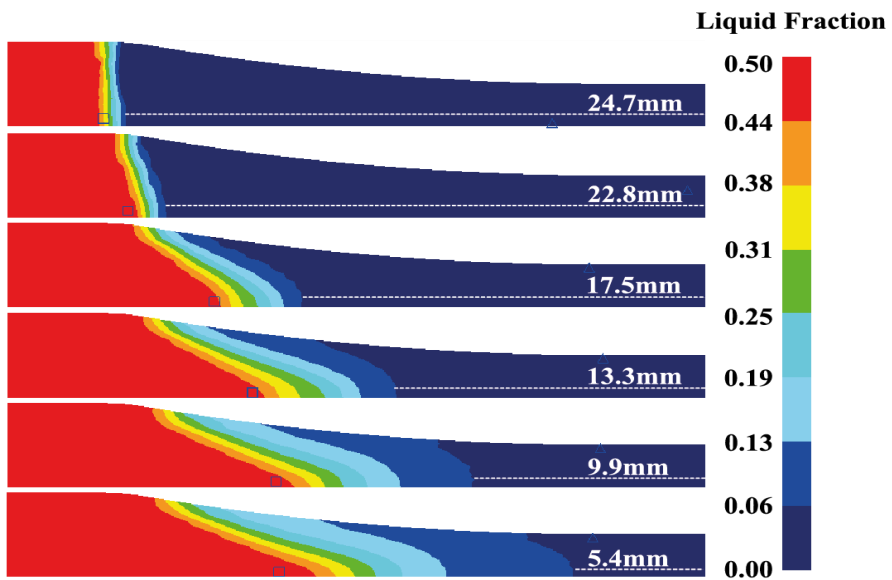


Figure 3.9 Liquid fraction distribution of Al-xMg binary alloys during the TRC process

3.3.3 FEM simulation of the solidification behavior during the TRC process of Al-4Mg alloy with different casting speeds

Various parameters can affect the solidification behavior during the TRC process such as melt temperature, melt loading weight, and casting speed. In current study, casting speed was chosen to study the effect of casting parameters on solidification behavior of high Mg (4%) alloyed Al alloy.

Fig. 3.10 shows the temperature distribution and liquid fraction distribution of Al-4Mg alloy during the TRC process under different casting speeds given by DEFORM simulated results. Simulation was carried out with different settings of casting speeds including 3.22 mpm, 2.92mpm, and 2.63mpm. From the results shown in Fig. 3.11, we can conclude that with higher casting speed less deformation region and longer depth of sump were calculated which can be explained by the less contacting time between melt and roll [6].

As mentioned in Fig. 3.3, specific points were selected and tracked during the TRC simulation to study the change across the thickness direction. Liquid fraction (see Fig. 3.10), strain in vertical direction (see Fig. 3.11), and strain in horizontal (see Fig. 3.12) direction were recorded at every points after 2s from the starting point of the TRC simulation to get stable condition.

Fig. 3.11 shows the liquid fraction along the thickness direction, center layer was observed to have more liquid compared to the fringe while with higher casting speed the remaining liquid was predicted to have larger fraction across the whole area. This can explain the usually observed macro-segregation in

the center layer of TRC strips that solution can be rejected to the remaining melt and form a solution enriched layer in the center part of the TRC strips.

Fig. 3.12 presents the strain in vertical direction while Fig. 3.13 shows the strain in horizontal direction at specific points during the TRC simulation, fringe part and center layer were predicted to have more compression deformation during the TRC process than the mid layer. In addition, shear deformation was found to be mainly active at the fringe part. Furthermore, while the casting speed increases, less strain in both vertical and horizontal direction was confirmed induced by the less contacting between roll and the melt.

3.4 Conclusion

Based on the simulation results using JMatPro and DEFROM software, the effects of alloying elements and casting speed on the solidification and deformation behavior of Al-Mg binary alloys were investigated. The main conclusions can be drawn as follows:

(a) Longer depth of sump and less deformation region were confirmed with more Mg addition induced by longer freeze range and lower thermal conductivity.

(b) Less deformation region was confirmed with higher casting speed and more remaining liquid was observed in mid-layer according to the simulation results. Moreover, more strain was predicted at center-layer compared to the mid/side layer during the TRC process.

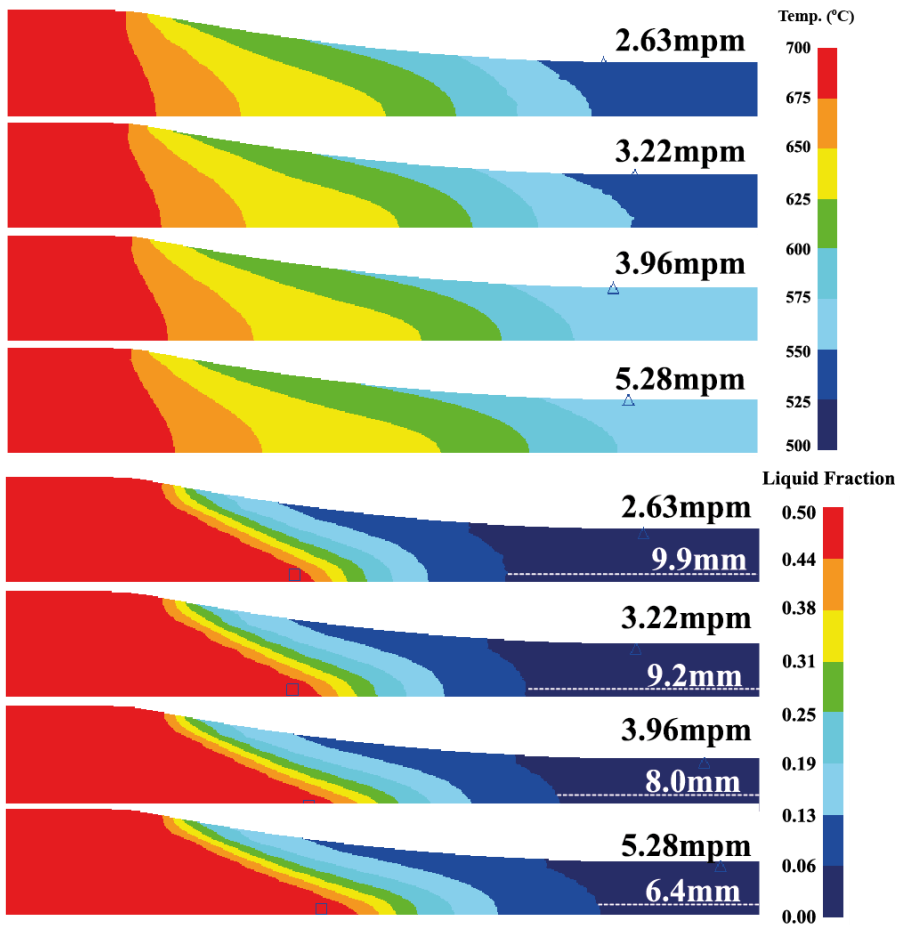


Figure 3.10 Temperature distribution and liquid fraction distribution of Al-4Mg binary alloy during the TRC process under different casting speeds.

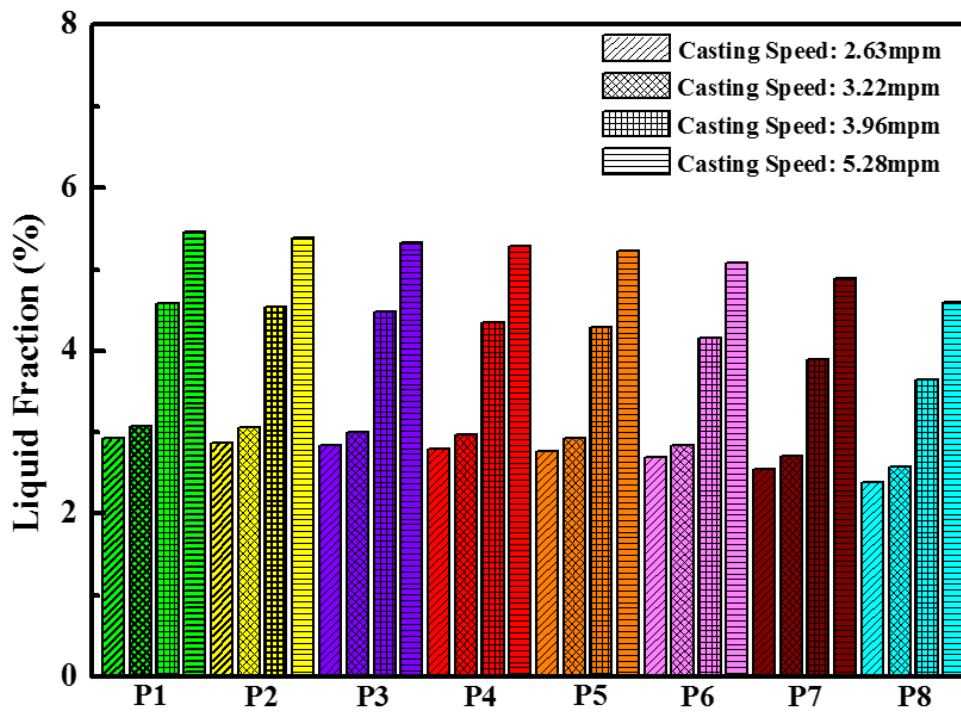


Figure 3.11 Liquid fraction at specific points during the TRC process.

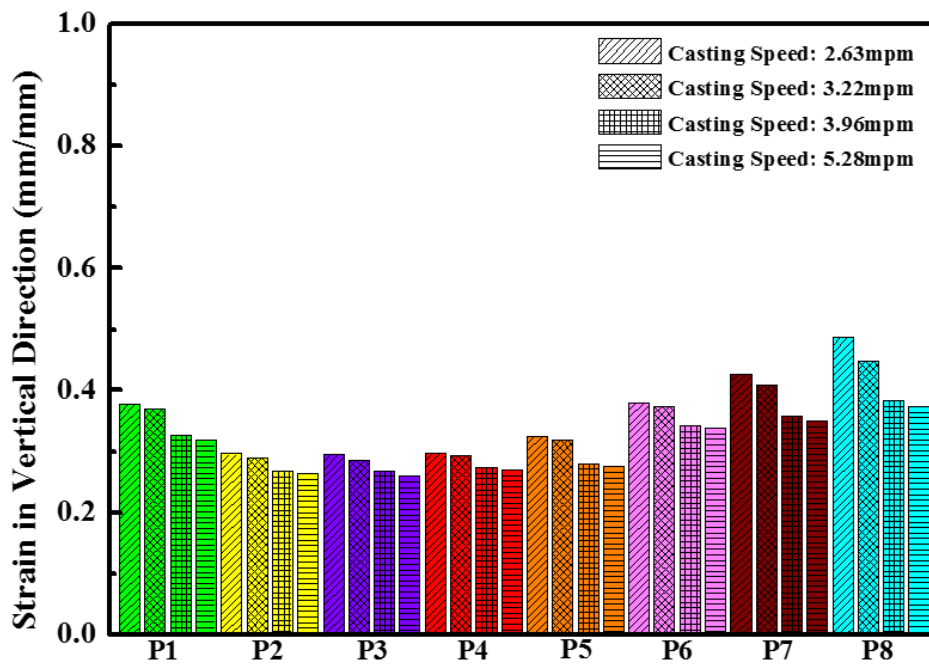


Figure 3.12 Strain in vertical direction at specific points during the TRC process.

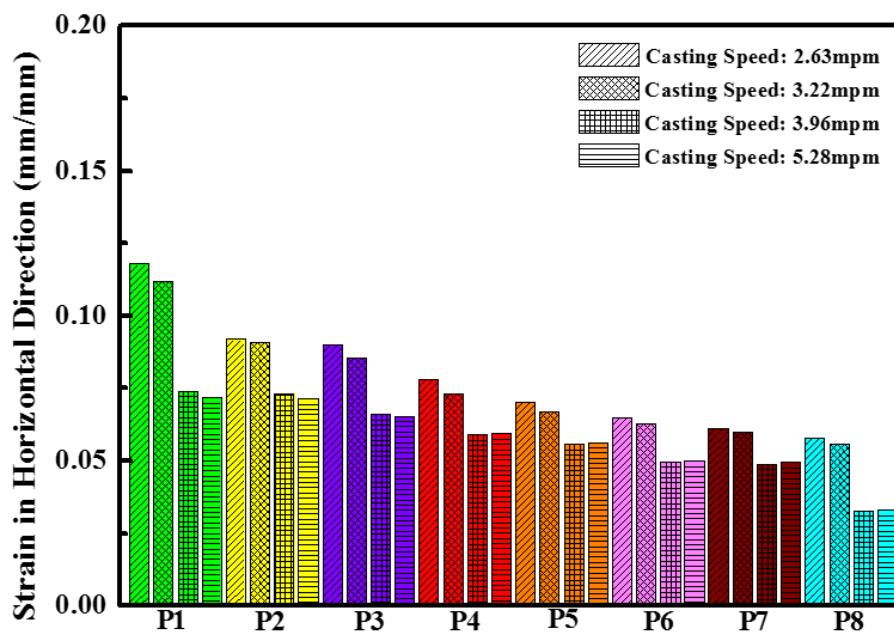


Figure 3.13 Strain in horizontal direction at specific points during the TRC process.

Bibliography

- [1] N.S. Barekar, B.K. Dhindaw, "Twin-roll Casting of Aluminum Alloys- An overview, Materials and Manufacturing Processes", 29(2014), 651-661.
- [2] S.J. Park, H.C. Jung, K.S. Shin, "Analysis of the Solidification and Deformation Behaviors of Twin Roll Cast Mg-6Al-X Alloys", Metals and Materials International, 22(2016), 1055-1064.
- [3] J.J. Park, "Finite-Element Analysis of a Vertical Twin-roll Casting", Metals and Materials International, 20(2014), 317-322.
- [4] J.J. Park, "Numerical Analysis of Horizontal Twin-Roll Casting for AA3003", Metallurgical and Materials Transactions A, 49(2018), 4748-4758.
- [5] Y. Birol, "Analysis of Macro Segregation in Twin-roll Cast Aluminum Strips via Solidification Curves", Journal of Alloys and Compounds, 486(2009), 168-172.
- [6] H. Zhao, P.J. Li, L. He, "Coupled Analysis of Temperature and Flow during Twin-roll Casting of Magnesium Alloy Strip", Journal of Materials Processing Technology, 211(2011), 1197-1202.

4. Effect of alloying elements and casting speed on internal macro-segregation of Al-Mg binary alloys during the TRC process

4.1 Introduction

Al-Mg binary alloy systems had been studied by researchers all around the world since Mg is one of the most important alloying elements of commercial Al alloys such as AA6xxx and AA5xxx series alloys [1]. The formation mechanism of two kinds of deformation induced center segregation in TRC Al-Mg strips was studied by M.S. Kim. A segregation band formed due to high compression rate and a periodic positive/negative center segregation formed during the distribution of remaining melt in the mid-layer [2]. M. Yun discussed the channel segregation, deformation segregation, and the banded structure in his study and gave the formation of mentioned segregation types. According to his analysis, channel segregation forms due to back flow of remaining Mg-rich melt while deformation segregation which is actually the same with the segregation band in M.S. Kim's research forms due to high compression rate. Besides, banded structure forms when sufficient solid exits and the inner layer was loaded with roll force which increase the heat transfer coefficient and help to form fine dendrite structure as a banded layer [3]. However, the formation of coarse structure inside the banded region stays

unclear.

4.2 Experimental

Al-Mg strips with Mg compositions of 0.5~5.0% were fabricated by twin-roll casting process (TRC) at different casting speeds. Pure Mg and Al ingots were mixed and melted before twin-roll casting and chemical compositions of strips were shown in Table 4.1.

The strips were prepared by a twin-roll caster shown with a constant roll gap. The caster consists of a pair of copper rolls with 140 mm in diameter with running water tunnels equipped inside. Springs were positioned between upper roll and caster frame to give enough roll force during the casting process while lower roll was fixed firmly. Ingots of ~3.0 kg were melted in a hot chamber and stirred for 10 minutes to get homogenized melt. A pendulum was brought down at a constant speed and pushed the melt coming out through a nozzle toward moving rolls with constant melt loads per unit time.

In the present work, strips were cast at 700°C with a melt loading weight of 4.79 kg/s*m. Initial roll force was set to 140kg and casting speed was assigned from 2.63mpm to 3.22mpm, see Table 4.2. Eventually, strips with a thickness of about 4mm and a width of about 63mm were prepared.

Extra experiments were carried out of Al-4Mg under various casting speed to help to understand the formation mechanism of various segregation types. Addition strips were cast under the same condition and the speed was assigned at 2.63mpm, 3.22mpm, 3.97mpm, and 5.28mpm.

Longitudinal cross-section at the center width layer was machined and mounted in a resin holder followed by continuous polishing. Polished longitudinal cross-sections were etched using a Keller's reagent etchant to show reveal the segregation and were anodized in a Barker's reagent under 20V for 3min to show the grain structure. Micro-structures of longitudinal cross-sections were examined by using an optical microscope and a scanning electron microscope (SEM). Distribution of Mg elements across thickness direction was measured by energy-dispersive X-ray Spectroscopy (EDAX).

Homogenization heat treatment was carried out for Al-4Mg alloys and grain structure after homogenization was observed as well. The tensile test samples were machined from as-cast strips and the tensile tests were performed according to the ASTM standard B557M using an Instron 5582. Tensile test loading direction was parallel to the casting direction.

Table 4.1 Chemical compositions of as-TRC binary Al-Mg alloys. (wt.%)

Alloys	Chemical Compositions (wt.%)			
	Mg	Si	Fe	Al
Al-0.5Mg	0.48	0.08	0.09	Bal.
Al-1.0Mg	0.92	0.05	0.03	Bal.
Al-2.0Mg	2.08	0.06	0.08	Bal.
Al-3.0Mg	2.82	0.06	0.07	Bal.
Al-4.0Mg	3.96	0.09	0.07	Bal.
Al-5.0Mg	5.29	0.08	0.11	Bal.

Table 4.2 Casting parameters and results of Al-Mg alloys

Alloys	Casting Parameters				Results	
	Melt Temperature (°C)	Initial Roll Force (Kg)	Melt Loading (kg/s*m)	Casting Speed (mpm)	Thickness (mm)	Width (mm)
Al-0.5Mg	700	140	4.79	3.22	3.62	~62
Al-0.5Mg	700	140	4.79	2.63	3.80	~59
Al-1.0Mg	700	140	4.79	3.22	3.26	~63
Al-1.0Mg	700	140	4.79	2.63	3.60	~62
Al-2.0Mg	700	140	4.79	3.22	3.24	~63
Al-2.0Mg	700	140	4.79	2.63	3.66	~61
Al-3.0Mg	700	140	4.79	3.22	3.33	~65
Al-3.0Mg	700	140	4.79	2.63	4.12	~60
Al-4.0Mg	700	140	4.79	3.22	3.45	~66
Al-4.0Mg	700	140	4.79	2.63	4.20	~60
Al-5.0Mg	700	140	4.79	3.22	3.41	~63
Al-5.0Mg	700	140	4.79	2.63	3.99	~62

4.3 Results and discussions

4.3.1 Effect of alloying elements on the internal macro-segregation of TRC Al-xMg strips

As shown in Table 4.2, strips with a length of about 2.5m and a width of 48mm to 66mm were fabricated. The thicknesses of fabricated strips differ from each other and show a relevance to casting speed. Strips cast at lower casting speed were found to have a larger thickness up to 4.20mm while high-speed cast strips were found to have much thinner thickness of about 3.40mm.

Microstructures of the longitudinal cross-section obtained from strips fabricated at different speeds were examined as shown in Fig. 4.1. Alloys with Mg less than 2% cast at lower speed (see Fig. 4.1 (b) and Fig. 4.1 (d)) were observed to have a uniform cross-section microstructure without any center segregations while alloys with Mg less than 2% cast at higher speed (see Fig. 4.1 (a) and Fig. 4.1 (c)) were confirmed to have a uniform microstructure with a slightly segregated center-layer.

Alloys with Mg more than 2% were observed to have a banded structure with a channel segregation in high-speed cast samples (see Fig. 4.1 (e), Fig. 4.1 (g), Fig. 4.1 (i), and Fig. 4.1 (k)). In addition, larger channel segregation area was found in samples with more Mg addition. In terms of alloys with Mg more than 2% in low-speed cast samples (see Fig. 4.1 (f), Fig. 4.1 (h), Fig. 4.1 (j), and Fig. 4.1 (l)), a highly deformed structure was observed and a vortex-shape segregation was found in the mid-layer with a slightly segregated center region. Generally, alloys with more Mg addition trend to form more

segregations.

Compared to the simulation results discussed in Chapter 3, experimental results in this study matched the predicted solidification behavior during the TRC process by DEFORM. Alloys with higher Mg addition have longer freeze range and lower thermal conductivity which indicate more remaining Mg-rich melt in the center layer and less heat transfer between the rolls and the melt (see Fig. 3.4, Fig. 3.5, and Fig. 3.6). Moreover, lower cooling rate induced by less contacting time between the roll and the melt at higher casting speed (see Fig. 3.10) which assist to the Mg-rich melt to remain in the mid-layer for longer time and form larger area of center-segregation (see Fig. 3.11). Less deformation caused by the larger depth of sump due to the increase of casting speed also help to explained the highly deformed structure with lower casting speed and banded structure with higher casting speed. The formation mechanism of banded structure will be discussed in next section along with other types of internal macro-segregation.

4.3.2 Effect of casting speed on the internal macro-segregation of TRC Al-4Mg strips

Extra experiments were carried out with Al-4Mg alloys cast at various speed. Table 4.3 shows the casting parameters and results. Thickness decreased with the increasing casting speed under same melt feeding rate. A maximum thickness of 4.20mm and a minimum thickness of 2.59mm were fabricated.

Microstructures of the longitudinal cross-section obtained from strips

fabricated at different speeds were examined as shown in Fig.4.2. Casting direction is from left to right. A highly deformed structure with a slight center segregation was observed in strips cast at 2.63mpm. Besides, a segregation layer was also found in this specimen as a vortex shape, see Fig.3.2 (a). Strips cast at 3.22mpm, 3.96mpm, and 5.28mpm showed a banded structure which has already been reported before [3,4]. Banded region in the mid-layer of twin-roll cast strips have a large area of fine structure with small secondary dendrite arm spacing which is totally different from columnar structure, see Figs. 4.2 (b,c,d) . However, some regions have coarser structure inside the middle banded region as shown in Fig. 4.2 (e) and become larger with the increasing casting speed, see Figs. 4.2 (c,d). Compared to strips cast at 3.96mpm and 5.28mpm, the strips with a casting speed of 3.22mpm showed a curved columnar structure indicating deformation during casting. Moreover, center-line segregations exist in all specimens with banded layer and were found located inside the banded region adjacent to coarser structure, see Fig. 4.2 (f).

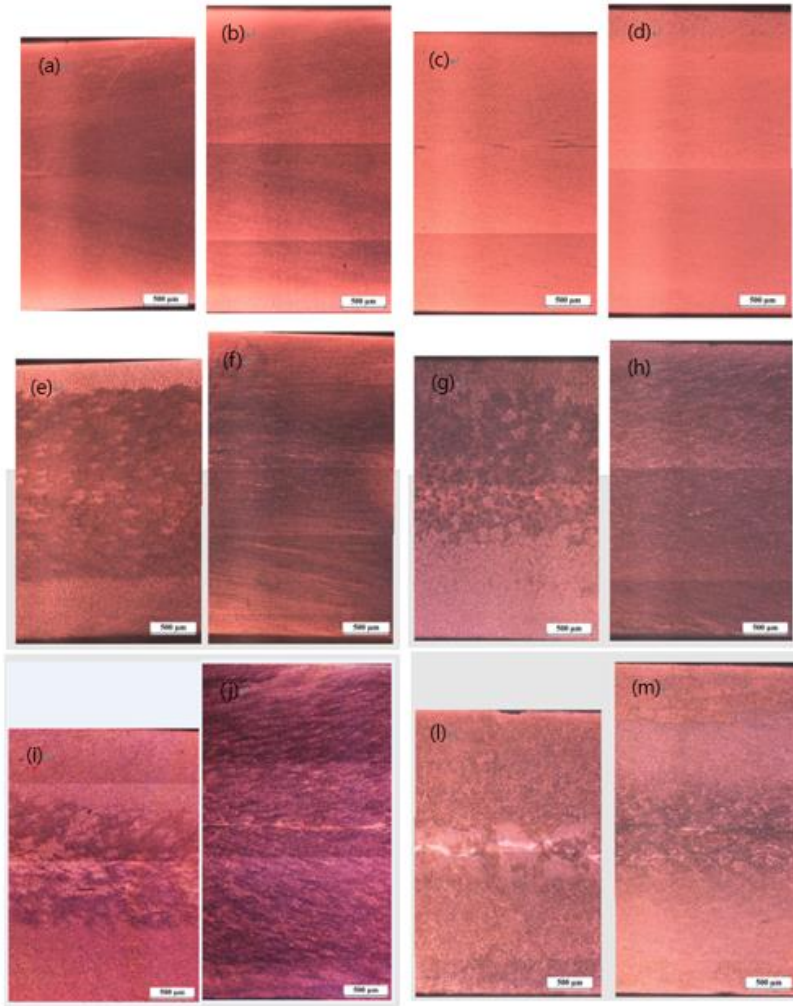


Figure 4.1 Microstructure of longitudinal cross-section of TRC Al-xMg alloys: Al-0.5Mg alloys cast at (a) 3.22mpm and (b) 2.63mpm; Al-1.0Mg alloys cast at (c) 3.22mpm and (d) 2.63mpm; Al-2.0Mg alloys cast at (e) 3.22mpm and (f) 2.63mpm; Al-3.0Mg alloys cast at (g) 3.22mpm and (h) 2.63mpm, Al-4.0Mg alloys cast at (i) 3.22mpm and (j) 2.63mpm; Al-5.0Mg alloys cast at (k) 3.22mpm and (l) 2.63mpm.

Table 4.3 Casting parameters and results of Al-4Mg alloys

Alloys	Casting Parameters				Results	
	Melt Temperature (°C)	Initial Separating Force (Kg)	Melt Loading (kg/s*m)	Casting Speed (mpm)	Thickness (mm)	Width (mm)
Al-4.0%Mg	700	140	4.79	2.63	3.45	~60
Al-4.0%Mg	700	140	4.79	3.22	4.20	~66
Al-4.0%Mg	700	140	4.79	3.96	2.70	~54
Al-4.0%Mg	700	140	4.79	5.28	2.59	~48

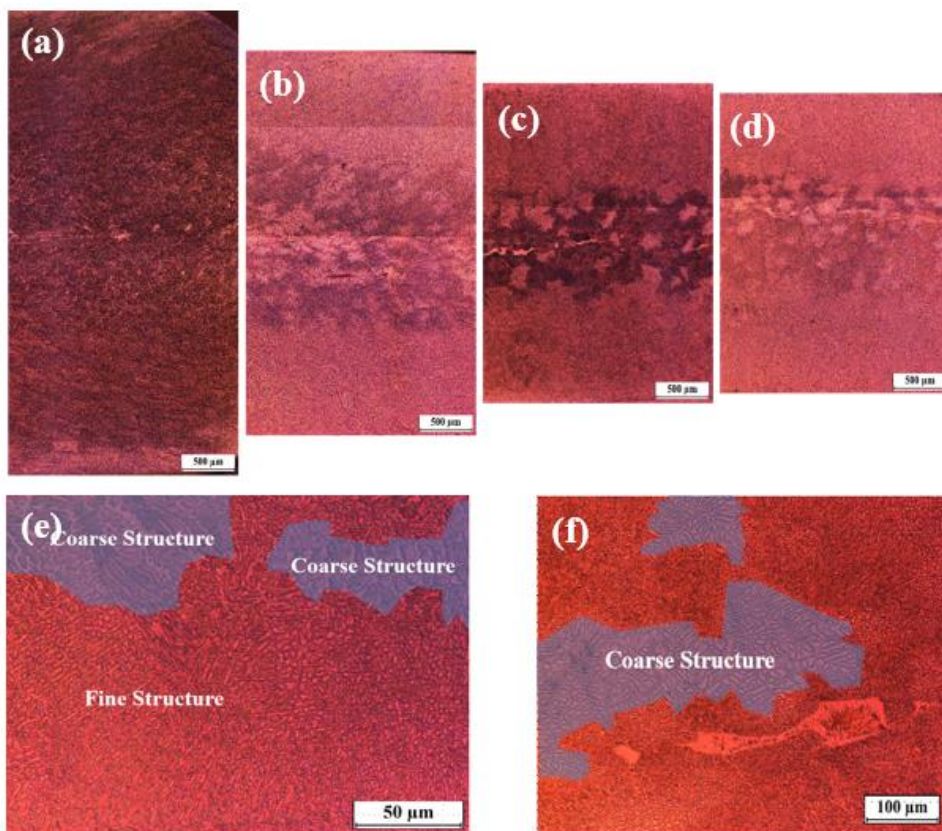


Figure 4.2 Microstructure of as-cast Al-4%Mg strips examined by an optical microscope under polarized light. Longitudinal Cross-section of strips cast at: (a) 2.63mpm, (b) 3.22mpm, (c) 3.96mpm, and (d) 5.28mpm. Banded Structure in strips cast at: (e) 3.96mpm and (f) 5.28mpm.

Since the difference of segregation intensity can make a great influence on properties, the distributions of Mg element in longitudinal cross-section of strips cast at 2.63mpm and 3.22mpm with 4% Mg were examined by EDAX and the results are shown in Fig. 4.3. A center-line segregation with periodic fibrous positive/negative segregation was found in high-speed (3.22mpm) cast strip which is composed of Mg-rich region and adjacent Mg-poor region along the longitudinal direction, see Fig. 4.3 (a). Mg element distribution was confirmed to be more homogenized and uniform in lower speed cast strip (2.63mpm), see Fig. 4.3 (b). Mg element change along thickness direction was measured and shown at Figs. 4.3 (c, d, e, f). Larger segregated aggregation and higher intensity were observed in high-speed cast strips while segregation with lower intensity was observed in low-speed cast strips. A large aggregated Mg-rich region was found as a positive segregation with an adjacent negative segregation, as shown in Fig. 4.3 (c).

As shown in Fig. 4.4, microstructure of segregation region in strips cast at 3.22mpm and 3.96mpm were observed (see Figs. 4.4 (a,b)) and grain structure of segregation region in strips cast at 2.63mpm was analyzed under a polarized light, see Fig. 4.4 (c). Channel segregations inside the banded layer of strips cast at 3.96mpm were found to be aggregated at the middle of the strips along thickness direction but with an oriented angle between each other which are different from the continuous channel segregation in previous research [2,3,5,6]. The negative segregation in 3.22mpm cast strip was confirmed as coarse dendrite structure inside the banded region as shown in

Fig. 4.4(b) and Fig. 4.3(c). In low speed cast strip, more uniform segregation structure was confirmed with lower intensity, as shown in Figs. 4.3 (d,f). Moreover, segregation was found to be located at severe deformed grain boundaries as shown in Fig. 4.4 (c).

FEGSEM micrographs of the segregation region in both 3.22mpm cast and 44mpm cast samples were presented in Fig. 4.5. A complex structure was observed in the positive segregation region of samples cast at 3.22mpm which was confirmed by EDAX point scanning, see Fig. 4.5(a). As shown on the composition scanning results, the composition of positive segregation region can be divided into two distinctive domains: A Mg-rich phase along with Fe and Si and a Mg-rich phase. In addition, negative segregation was confirmed with a binary composition of 1.25% Mg concentration, Fig. 4.5(b) shows the segregation structure in 2.63mpm cast sample. Only Mg-rich phase without other elements was found in the inter-dendrite region.

Fig. 4.6 shows the grain structure of Al-4%Mg alloys under a polarized light after anodization. Elongated structures which can be usually seen in as-rolled materials were observed in samples cast at 2.63mpm and 3.22mpm, see Figs. 4.6(a,b). Larger grains were found in samples cast at higher speed, see Fig. 4.6(a,b,c). The angle between the columnar angle and horizontal direction decreases with the increasing casting speed.

As-TRC strips with 4%Mg cast at 2.63mpm and 3.22mpm were homogenized at 400°C for 30min and 12h. The grain structure of as-cast

samples and as-homogenized samples were investigated and shown in Fig. 4.7. After homogenization for 30min, recrystallized structure was observed with the segregation region, see Fig. 4.7(b,e). While, center segregation was removed in both samples cast at 2.63mpm and 3.22mpm after homogenization for 12h, see Fig. 4.7(c,f). Since the strips were deformed during the TRC process, rolled structure recovered and recrystallized during the homogenization. Compared to the sample cast at 3.22mpm, much finer equiaxed grains were observed in the sample cast at 2.63mpm. Average grain size of the strips cast at 3.22mpm was confirmed to be about $150 \pm 90\mu\text{m}$. In contrast, an average grain size of $18\pm 9\mu\text{m}$ was observed in the strip cast at 2.63mpm.

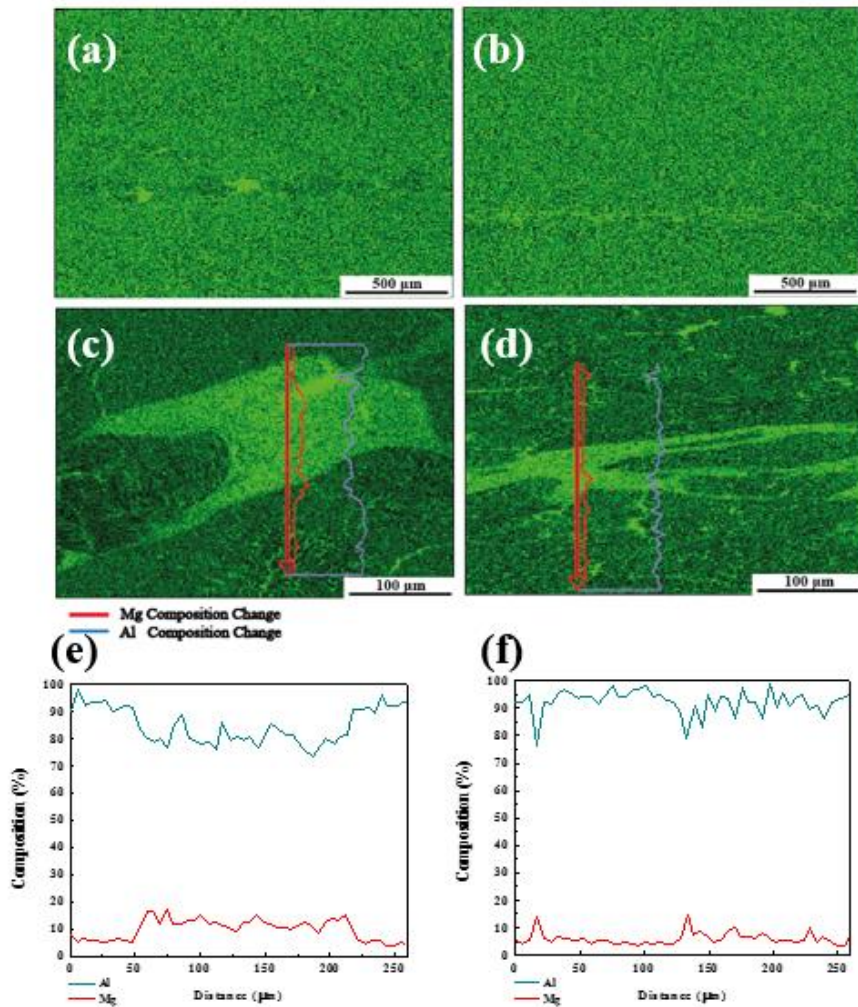


Figure 4.3 Mg element distribution in longitudinal cross-section of strips cast at: (a) 3.22mm and (b) 2.63mm; The concentration of Mg element changes along thickness direction of strips cast at: (c) and (e) at 3.22mm and (d) and (f) at 2.63mm

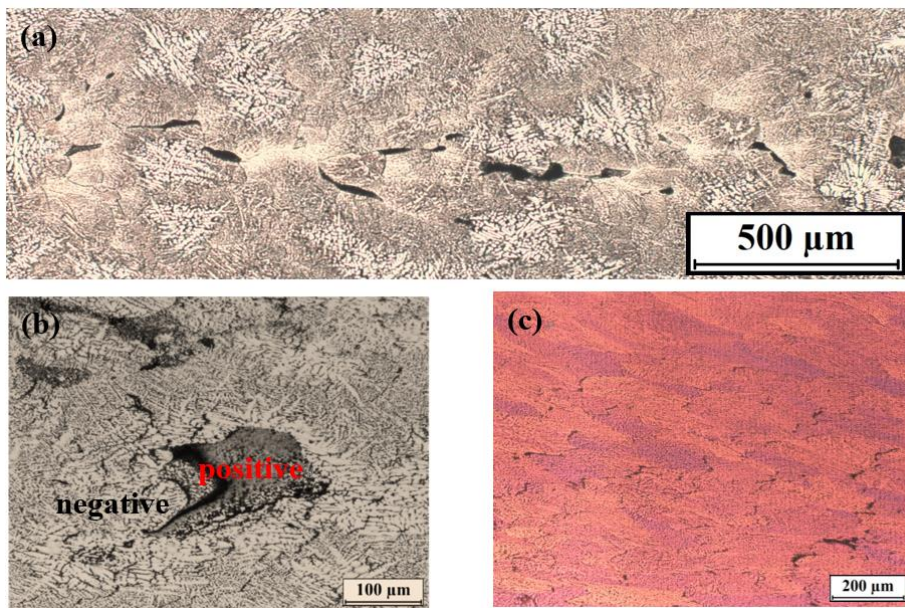


Figure 4.4 Micro-structure of segregation region in strips cast at: (a) 3.96mpm, (b) 3.22mpm, and (c) 2.63mpm (under polarized light)

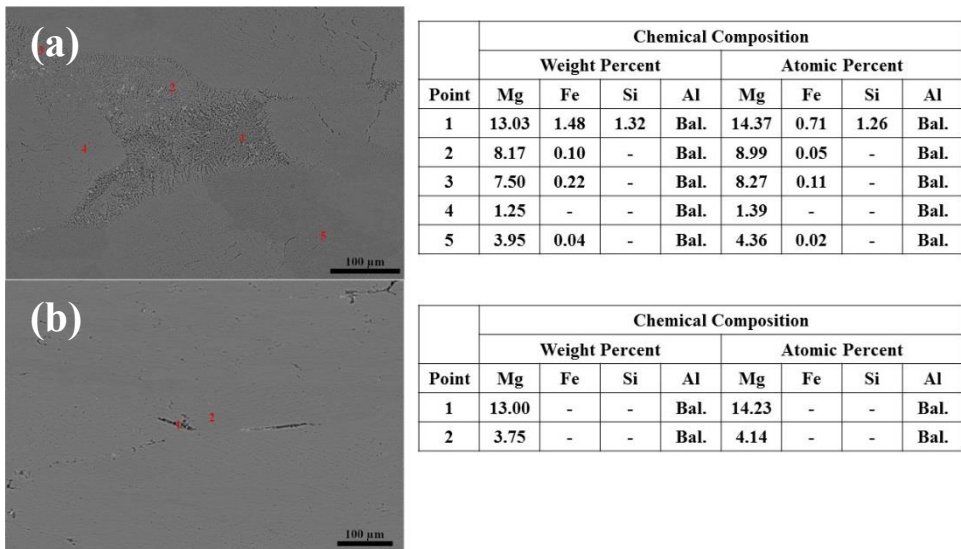


Figure 4.5 FEGSEM micrographs and EDAX point scan results of the segregation region in as-TRC samples cast at: (a) 3.22mpm and (b) 2.63mpm

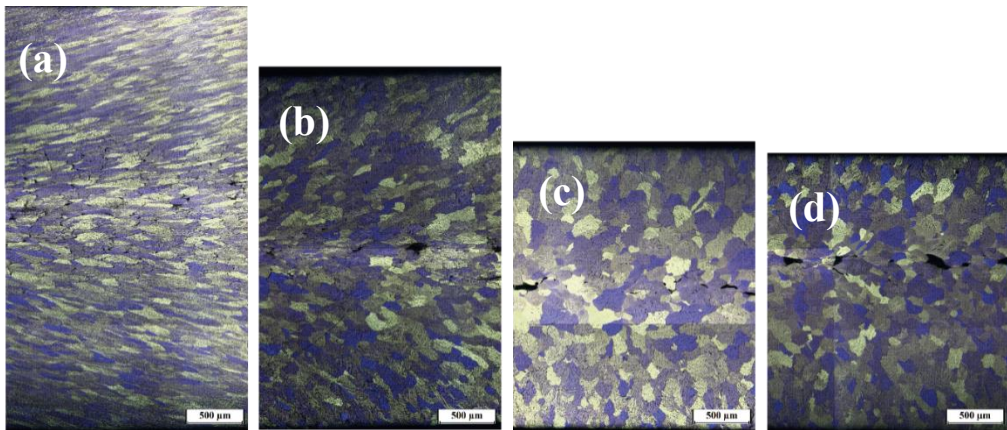


Figure 4.6 Grain structures of as-cast Al-4%Mg strips examined by an optical microscope under polarized light. Longitudinal cross-section of strips cast at: (a) 2.63mpm, (b) 3.22mpm, (c) 3.96mpm, and (d) 5.28mpm.

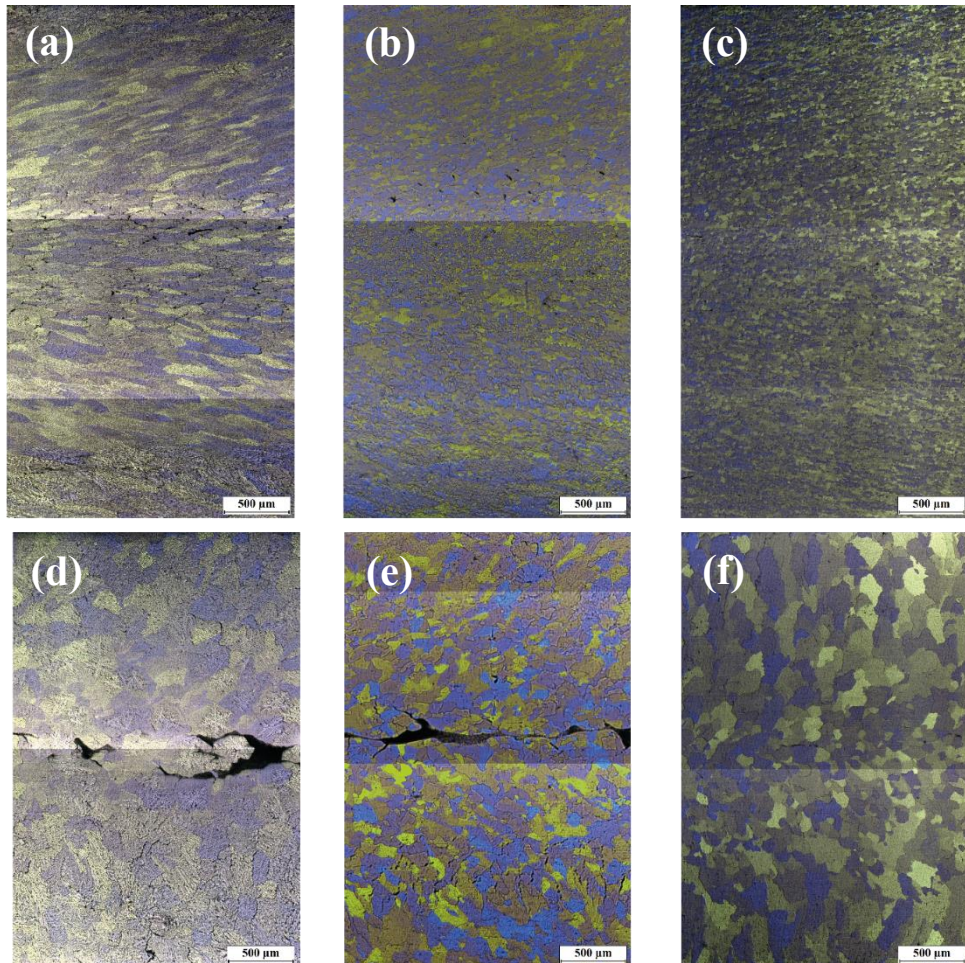


Figure 4.7 Grain structure of as-cast and as-homogenized TRC Al-4%Mg strips by an optical microscope under polarized light. Longitudinal cross-section of strips cast at: (a) as-TRC cast at 2.63mpm, (b) as-homogenized(30min) strip cast at 2.63mpm, (c) as-homogenized(12h) strip cast at 2.63mpm, (d) as-TRC cast at 3.22mpm, (e) as-homogenized(30min) strip cast at 3.22mpm, (f) as-homogenized(12h) strip cast at 3.22mpm,

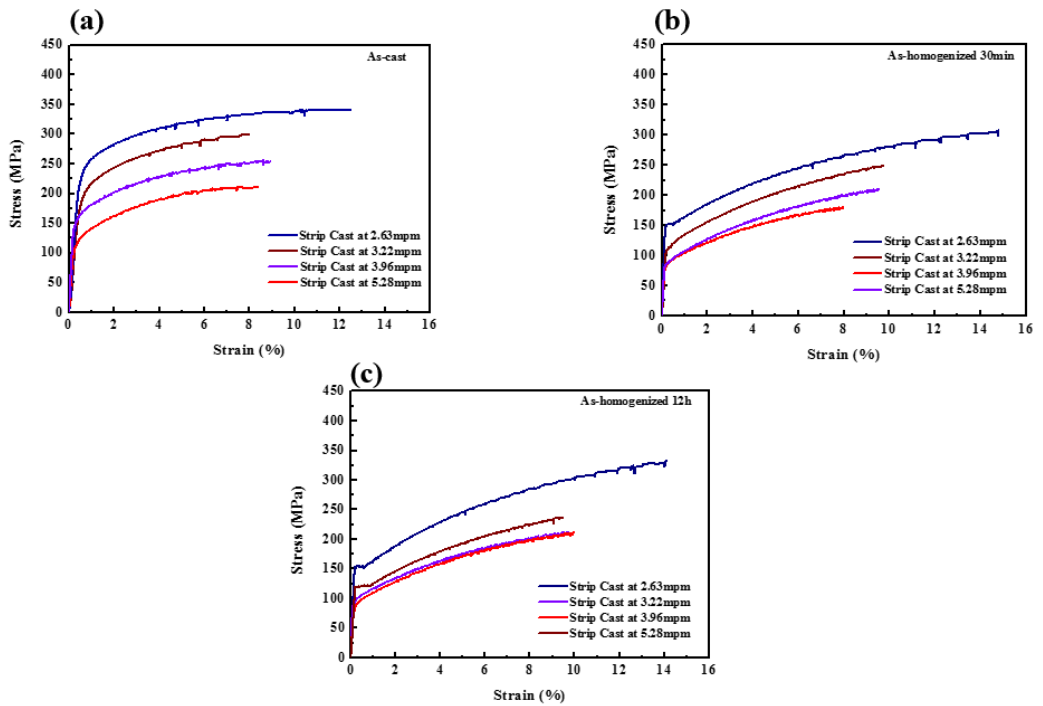


Figure 4.8 Strain-stress curves of: (a) as-cast samples, (b) samples homogenized for 30min, and (c) samples homogenized for 12h.

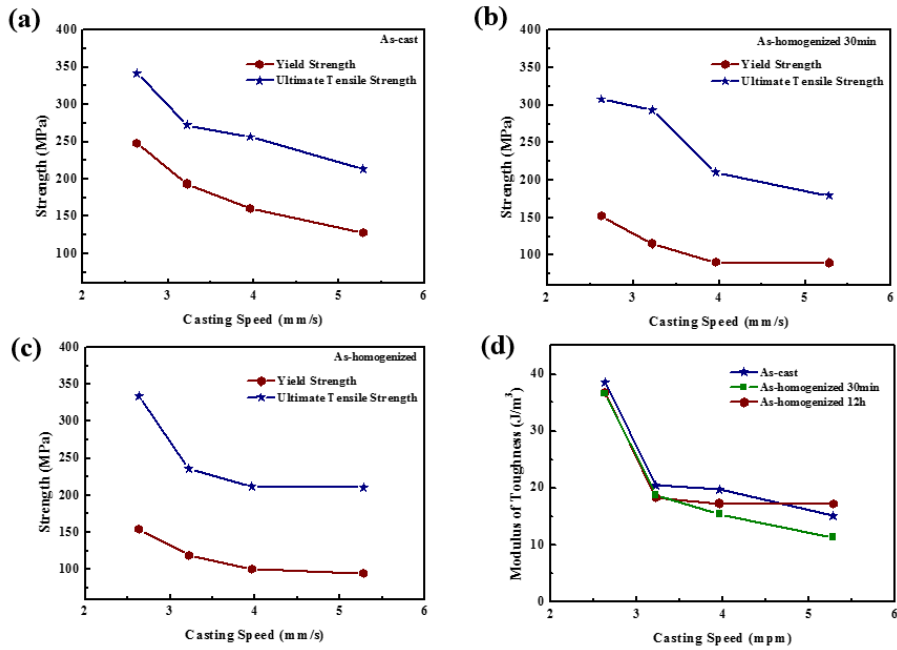


Figure 4.9 Mechanical properties of as-TRC strips cast at different speeds: (a) shows the relation between strength and casting speed of as-cast strips, (b) shows the relation between strength and casting speed of as-homogenized (30min) strips, (c) shows the relation between strength and casting speed of as-homogenized (12h) strips, (d) shows the relation between modulus of toughness and casing speed of as-cast and as-homogenized strips.

As shown in Fig. 4.8 and Fig.4.9, both strength and elongation of lower speed cast as-cast strips were confirmed to be higher than high-speed cast strips in both as-cast and as-homogenized strips. A YS of 237MPa and a UTS of 340MPa were obtained from the low-speed cast strips (Fig. 4.9(a)). However, both strength and elongation of high-speed as-cast strips decreased after homogenization while a decreased YS and similar UTS were found in as-homogenized samples cast at 2.63mpm (Fig. 4.9). Besides, YS and UTS decreased with increasing casting speed in both as-cast and as-homogenized samples. Despite samples cast at 2.63mpm, the interval of the strength of samples with different casting speed decreased and showed a gentle downtrend after homogenization for 12h. Compared to the properties of strips homogenized for 30min, the gap of the strength of strips decreased. In addition, the relation between the casting speed and the modulus of toughness was constructed and showed that toughness of material decreased with increasing casting speed (Fig. 4.9(d)). Similarly, except for 2.63mpm cast strips, the toughness decreased after homogenization and became analogous to each other.

4.3.3 Discussion of the formation mechanism of different segregation types and the effect of segregation behavior on final properties in current study

Casting speed was chosen as the main variable in this research. High casting speed reduces the contacting time between the roll and melts which results in lower cooling rate and longer depth of sump. This had been

supported by both experimental results [7] and numerical study [8]. Usually, it has been reported that with higher casting speed more liquid remains and larger segregated phases trend to be detected in the mid-layer region [9].

When the casting speed reaches a specific value, it can form a banded structure compared to common center-line structure [3,7]. It's quite clear that banded structure formed since enough melt solidified near the base of sump. And roll separating force played a major role in increasing pressure between two rolls which lead to larger heat-transfer coefficient [3,6]. However, there was no clear theory to explain the formation of coarser structure inside the banded region. M. Yun indicated the re-melting and recirculation of melt occur in mid-layer of strips may be a possible reason of the formation of those coarse structures [3]. J.J. Park predicted melt flows in the filling stage of the TRC process, and a flow vortex was found in the mid-layer induced by separating force from roll [14]. Remaining liquid can be forced to flow back to the sump induced by high roll separating force. According to experimental results in this study, with larger casting speed larger area of coarse structure was observed in strips cast at 3.96mpm and 5.28mpm. With higher casting speed, the back-flow velocity increase and the solidification in the mid-layer will be delayed. Some soft and unsettled inner banded grains may be squeezed back to inter-dendrite space resulting from thermal-contraction and originally form coarse structure. Larger area of coarse structure in high speed cast strips can be explained by the higher back-flow speed induced by higher casting rate.

Center-line segregation was observed in strips with higher casting speed. An Mg-rich region was confirmed in the segregation part and also Mg-poor area was found inside center-line segregation adjacent to the Mg-rich zone which was confirmed as a coarse dendrite structure, see Fig. 4.3 (c) and Fig. 4.4 (b). During twin roll casting, dendrite structures at the fringe part of strips were compressed. Solidified grains at the fringe part meet in the center layer and the remaining liquid could be pushed into the inter-dendrite region. Remaining melt was given enough time for further reaction to form Al-Mg-Fe-Si phase (see Fig. 4.5(a)) and remaining melt was squeezed from the inter-dendrite region to form positive segregation while α -phase with lower Mg concentration formed as a negative segregation, explaining negative segregation exist as coarse structure next to the positive segregation. This Also, M.S. Kim carried out TRC of high Mg Al-Mg alloys and found various segregation types induced by deformation which implied lower compression rate give enough time for semi-solid shells to encounter with each other and allow periodic fibrous positive/negative segregation lines formed since remaining liquid was squeezed toward the adjacent region in the mid-layer [2].

Segregation area was observed in strips with lower casting speed which has a uniform vortex shape. Vortex shape segregation observed in our research (Fig. 4.2 (a) & Fig. 4.4 (c)) formed during the vortex flow in the filling stage. Lower casting speed with same melt loading pushed the solidified grains and dendrites at the fringe and mid-layer space was compressed. Mg-rich liquid flowed backward due to the lack of space for accommodation and the back-

flowed liquid was driven by separating force to form a vortex flow in the melt filling stage [3]. Mg-rich melts were squeezed and flowed into inter-columnar space. Furthermore, columnar structures were distorted and some grains were tilted (see Fig. 4.4(c) grain structure observed under polarized light), between which was filled with remaining Mg-rich melt and finally form a vortex shape segregation, see Fig. 4.4 (c).

Tensile tests of as-cast strips were carried out and strips fabricated by lower casting speed had both higher strength and ductility, see Fig. 4.9. The reason could be complicated. Segregation and remaining strain after deformation may affect the final mechanical properties. As shown in Fig. 4.8, segregation was removed in both high-speed cast and low-speed cast strips after homogenization for 12h while segregation was still found along with a recrystallized structure after homogenization for 30min. When we compare the properties of both homogenized samples for 30min and 12h, properties became similar when the segregation was removed in all high-speed cast samples. From which we can conclude that, the initial mechanical properties are related to the segregation structure. Moreover, a super fine grain structure was observed in as-homogenized strips cast at 2.63mpm. Mechanical properties after homogenization showed decreased YS, UTS, and modulus of toughness with more similar properties in strips cast at higher speeds. Since the residual stress relaxation and segregation reduction occurred during the homogenization, apparent differences in mechanical properties of as-cast strips were mainly affected by center-line segregation and banded structure

formed during the TRC process. In terms of strips cast at 2.63mpm, lower casting speed offered higher cooling rate which resulted in longer deformation region during the TRC process. The stored strain energy became the nuclei for recrystallization and formed a super fine grain structure which contributed to the sound mechanical properties after homogenization.

4.4 Conclusion

Addition of Mg trends to form larger fraction of internal macro-segregation. Types of center segregation changed with different casting speeds. Internal macro-segregations occur in the center layer of Al strips were influenced by solidification and deformation.

(a) Banded structure formed since sudden increase of heat-transfer coefficient, and coarse structure inside banded region caused by melt recirculation due to vortex melt flow.

(b) Internal macro-segregation was influenced by both deformation and melt flow which vary with different casting conditions.

(c) More uniform vortex shape segregation formed by the severe deformation during the TRC process which pushed remaining melt to flow back and finally segregated at the inter-dendrite/grain region.

(c) Better mechanical properties were found in strips with uniform vortex segregation fabricated at lower casting speed. And super fine grain structure was also observed in strips cast at lower casting speed.

Bibliography

- [1] R.S. Rana, R. Purohit, S. Das, “Reviews on the Influences of Alloying Elements on the Microstructure and Mechanical Properties of Aluminum Alloys and Aluminum Alloy Composites”, *International Journal of Scientific and Research Publications*, 6(2012), 2250-2257.
- [2] M.S. Kim, S.H. Kim, H.W. Kim, “Deformation-induced Center Segregation in Twin-roll Cast High-Mg Al-Mg Strips”, *Scripta Materialia*, 152(2018), 69-73.
- [3] M. Yun, S. Lokyser, J.D. Hunt, “Twin roll casting of aluminum alloys”, *MSE A*, 2000, pp.116-123.
- [4] N.S. Barekar, B.K. Dhindaw, *Twin-roll Casting of Aluminum Alloys-An overview*, *Materials and Manufacturing Processes*, 2014, pp.651-661.
- [5] K.H. Kim, The effect of melt conditioning on segregation of solute elements and nucleation of aluminum grains in a twin roll cast aluminum alloy, *Metallurgical and Materials Transactions A*, 2014, pp.4538-4548.
- [6] S.A. Lockyer, M. Yun, J.D. Hunt, D.V. Edmonds, Micro- and macrodefects in thin sheet twin-roll cast aluminum alloys, *Materials Characterization*, 1996, pp.301-310.
- [7] K.M. Sun, L. Li, S.D. Chen, G.M. Xu, G. Chen, R.D.K Misra, G. Zhang, A new approach to control centerline macrosegregation in Al-Mg-Si alloys during twin roll continuous casting, *Materials Letters*, 2017, pp.205-208.

[8] J.J. Park, Numerical analysis of horizontal twin-roll casting for AA3003, The Minerals, Metals & Materials Society and ASM International, 2018, pp.4748-4758

[9] S.J. Park, H.C. Jung, K.S. Shin, Analysis of solidification behaviors of twin roll cast Mg-6Al-X alloys, Metals and Materials International, 2016, pp.1055-1064.

5. Effect of casting parameters on internal macro-segregation of commercial AA6016 alloy

5.1 Introduction

The heat treatable 6xxx series alloys have wide application of automotive outer skin panel where high strength, high formability, and lower fabrication cost [1]. Nowadays, 6xxx series are gaining sound properties owing to the age hardening especially the paint-bake hardening at around 160~180°C for a short period [2,3]. Twin-roll casting as an applicable process to fabricate Al alloys with a high productivity and lower price, has great potential for further application [4]. Both solidification and deformation may occur in the TRC process, and the initial structure of as-TRC alloys make a great influence on the following thermal-mechanical processes including heat-treatment and cold working [5].

Internal macro-segregation in TRC Al alloys have a detrimental impact on the subsequent processing and properties of cast materials. Moreover, macro-segregation is difficult to be totally removed through the following processing after the solidification [6]. Accordingly, fabrication of commercial Al alloys with excellent qualities and segregation free structure is a great challenge lies ahead.

C. Gras investigated the segregation behavior of Al alloys during the TRC

process and created a defect free map of Al-Mg-Mn alloys based on the experimental results [7]. Buckling limit diagrams of AA1080, AA3004, AA5052, and AA8011 alloys were defined and the defect limit diagram of AA6111 was confirmed by S.A. Lockyer [8]. However, no sufficient information about AA6016 commercial alloy has been introduced to help casting parameters optimization in mass production.

5.2 Experimental

As presented in Table 5.1, 13 different casting parameters were configured to obtain strips of different thickness. In the present work, strips were cast at 700°C with various melt loading weights. Initial roll force was set about 130~140kg and casting speed was assigned from 2.4mpm to 4.4mpm. Eventually, strips with a thickness of 2.4~4.8mm were successfully fabricated. Longitudinal cross-section at the center width layer was carefully polished and etched using a Keller's reagent etchant to show reveal the segregation. Microstructures of longitudinal cross-sections were examined by using an optical microscope.

Internal channel segregation area indexes of different samples were calculated with a commercial image threshold program ImageJ. The thicknesses of cast strips were correlated with loading weight and casting speed to examine the dominating parameters for thickness control. Finally, channel segregation free diagram was defined based on the loading weight and thickness of AA6016 alloy.

Table 5.1 Casting parameters and results of AA6016 alloys

No	Casting Parameters				Results		
	Melt Temperature (°C)	Initial Roll Force (Kg)	Casting Speed (mpm)	Melt Loading (kg/s*m)	Thickness (mm)	Width (mm)	Channel Segregation Area (%)
1	700	140.5	3.0	4.19	3.9	57	0.8037
2	700	134.6	3.0	4.87	3.8	57	-
3	700	140.5	3.0	4.79	3.6	58	1.707
4	700	140.5	3.5	4.16	3.2	57	1.451
5	700	142.5	3.5	4.31	3.1	55	1.543
6	700	128.7	2.6	5.07	4.2	57	-
7	700	138.5	2.6	5.35	4.1	54	-
8	700	142.5	3.9	4.32	2.9	57	1.211
9	700	144.4	3.9	4.40	2.9	56	1.089
10	700	132.6	2.4	4.92	4.8	52	-
11	700	136.6	2.4	4.73	4.2	54	-
12	700	144.4	4.4	4.16	2.3	57	0.327
13	700	146.5	4.4	4.31	2.4	55	0.705

5.3 Results and discussions

The loading weight/thickness curve and casting speed/thickness curve were constructed, different fitting methods were used to find the best fit which can transform the ordinary non-linear data points into a linear relation. As shown in Fig.5.1 (b), a linear relation between thickness and casing speed was fitted which indicates that compared to loading weight, casting speed is a dominating influence on thickness.

Microstructures of longitudinal cross-section of TRC strips were observed and shown in Fig.5.2. Uniform structure was observed in alloy No.2,6,7,10,11 while channel segregation structure was examined in alloy No.1,3,5,8,9,12,13. Accordingly, channel segregation free diagram was constructed and shown in Fig.4.3. As shown in Fig. 5.3, strips cast under high-feeding & thickness condition were confirmed to have channel free structure with a more uniform structure, while low-feeding & thickness strips were found to form less segregation compared to average-feeding & thickness condition in the obtained diagram. This can be explained by the formation mechanism of internal macro-segregation in Chapter 4, channel segregation forms when the solidified shell meet and encounter with each other accompanied by the compression of the mid-layer space, remaining melt flew and redistribute in the mid-layer region. Moreover, when the melt is loaded at a lower level, striped solidified rapidly owing to the small

amount of melt which help to form less channel segregation.

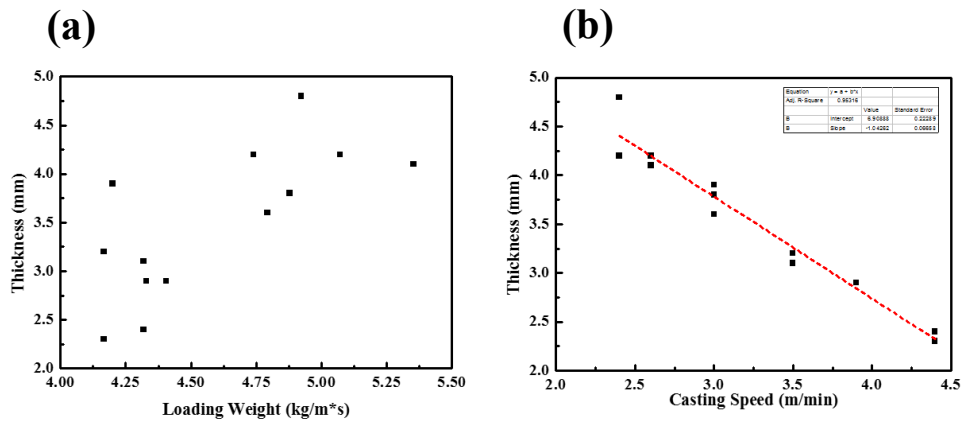
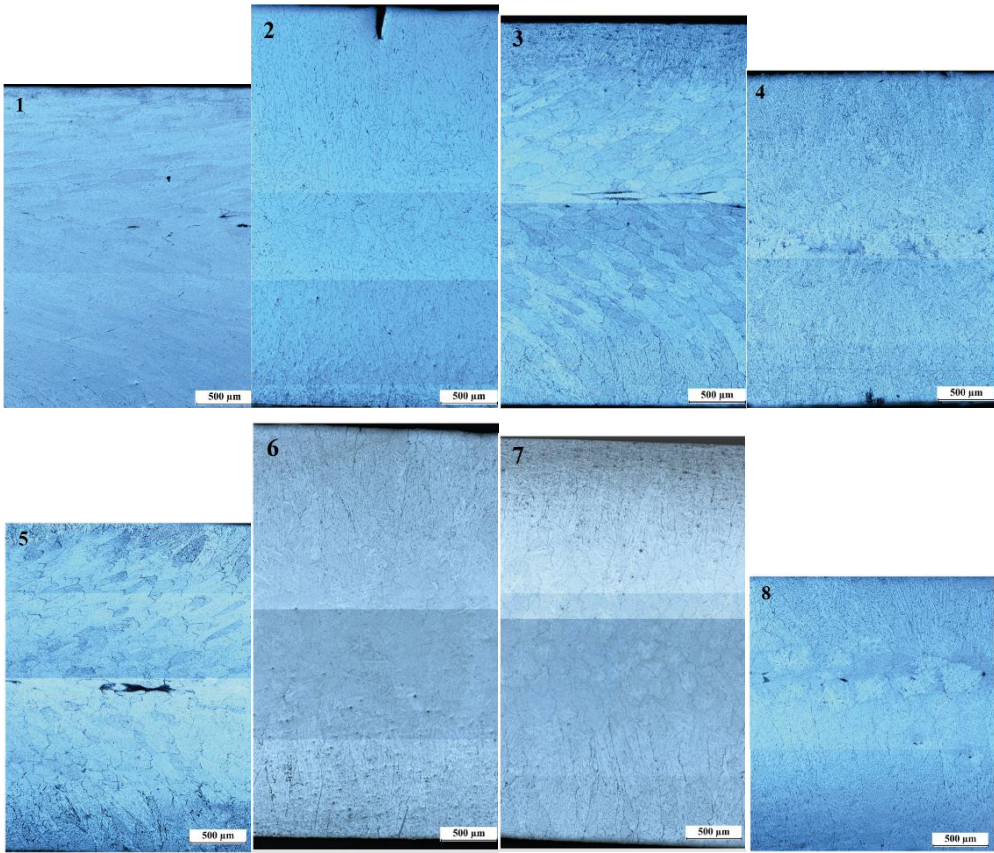


Figure 5.1 (a) loading weight-thickness curve and (b) casting speed-thickness curve constructed with experimental results.



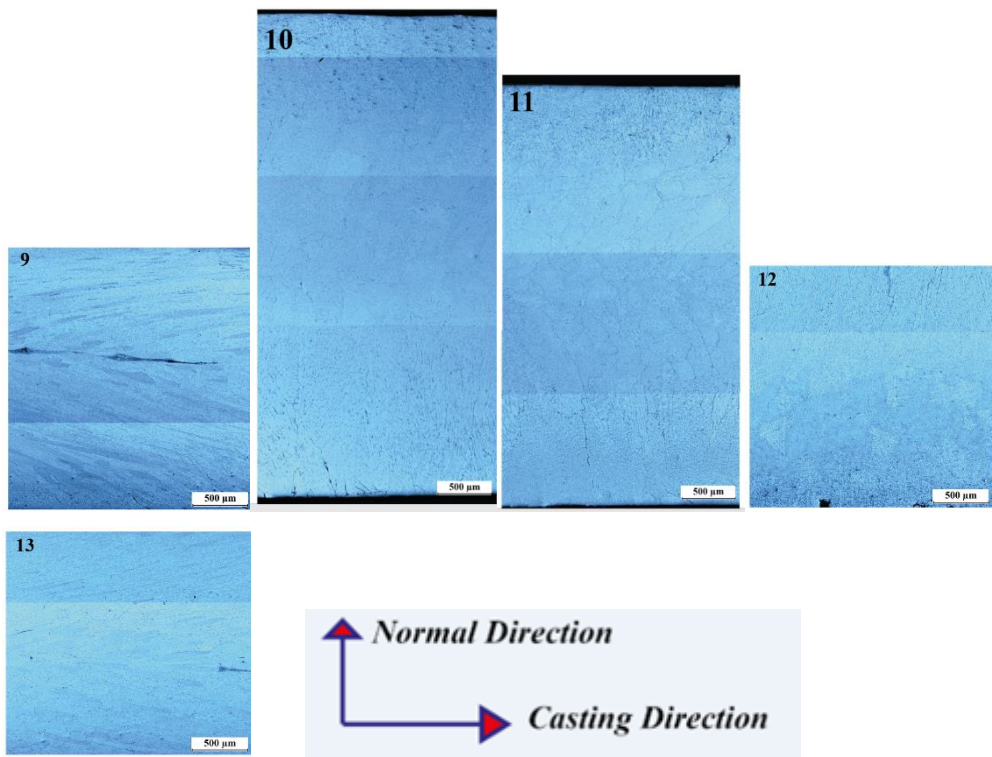


Figure 5.2 Microstructure of longitudinal cross-section of as-TRC AA6016 alloy.

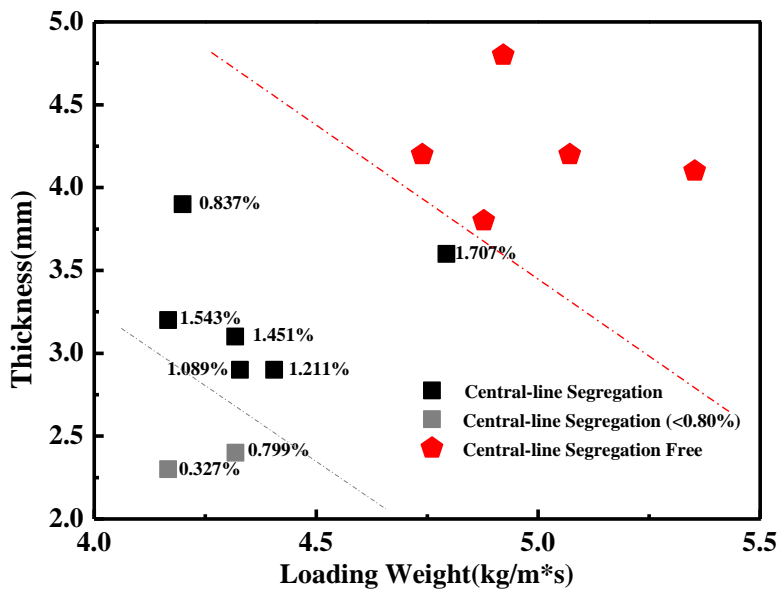


Figure 5.3 Channel segregation free diagram of AA6016 alloy during the TRC process.

5.4 Conclusion

13 different casting parameters were assigned to investigate the optimized casting parameters of AA6016 commercial alloy. Microstructures of longitudinal cross-section of as-TRC strips were observed. Subsequently, the channel segregation free diagram was constructed which indicated that:

(a) High-feeding & thickness condition can help to obtain more uniform structure without channel segregation.

(b) Strips cast under low-feeding & thickness conditions were found to have less channel segregation owing to faster solidification than average-feeding & thickness condition.

Bibliography

- [1] S.M. Hirth, G.J. Marshall, S.A. Court, D.J. Lloyd, "Effect of Si on The Aging Behavior and Formability of Aluminum Alloys Based on AA6016", *MES A*, 319(2001), 452-456.
- [2] T. Moons, P. Ratchev, P. DeSmet, B. Verlinden, P.V. Houtte, "A Comparatively Study of Two Al-Mg-Si Alloys for Automotive Applications", *Scripta Materialia*, 35(1996), 939-945.
- [3] A. Perovic, D.D. Perovic, G.C. Weatherly, D.J. Lloyd, "Precipitaion in Aluminum Alloys AA6111 and AA6016", *Scriptia Materialia*, 41(1999), 703-708.
- [4] Y. Birol, "Twin-roll Cast Al-Mg-Si Sheet for Automotive Applications", *Zeitschrift Fur Metallkunde*, 95(2004), 381-386.
- [5] T. Mizoguchi, K. Miyazawa, "Formation of Solidification Structure in Twin Roll Casting Process of 18Cr-8Ni Stainless Steel", *ISIJ International*, 35(1995), 771-777.
- [6] O. Daaland, A.B. Espedal, M.L. Nedreberg, I. Alvestad, "Thin Gauge Twin-roll Casting, Process Capabilities and Product Qualities", *Essential Readings in Light Metals*, (2016), 989-996.
- [7] C. Gras, M. Meredith, J.D. Hunt, "Microdefects Formation during The Twin-roll Casting of Al-Mg-Mn Aluminum Alloys", *Journal of Materials Processing Technology*, 167(2005), 62-72.

[8] S.A. Lockyer, M. Yun, J.D. Hunt, D.V. Edmonds, “Micro – and Macrodefects in Thin Sheet Twin-roll Cast Aluminum Alloys”, *Materials Characterization*, 37(1996), 301-310.

6. Final conclusion

Based on all simulation and experimental data presented and discussed above, conclusion can be drawn as follows:

(a) Types and area fraction of segregation are effective to alloying elements and casting parameters in TRC process.

(b) With higher Mg additions, thicker remaining melt layer accommodates in the center layer of the TRC strips before the final solidification and causes thicker segregation layer in the final strips.

(c) Casting speed makes a great influence on the segregation behavior of TRC strips. With lower casting speed, the contacting time between melt and roll increases which allows more heat transfer between them and results in a faster cooling rate according to the simulation results. When the casting speed is exceedingly low enough, a vortex-shape structure forms induced by rapid cooling rate and circulating flow of melt in the center and mid layer of the melt. While, faster cast samples have a banded structure with channel segregation inside indicating more melt re-circulation and lower cooling condition.

(d) Initial microstructure and segregation affect the mechanical properties of as-TRC samples. Samples with a highly deformed vortex-shape structure has better properties which can be explained by less segregation, finer grain structure and work hardening.

초록

알루미늄 합금은 낮은 밀도, 높은 강도 및 우수한 부식 저항성을 지니고 있어 구조재료로서 산업에 적용되고 있다. 하지만 철강 보다 비싼 생산 원가로 인하여 적용 범위가 국한된다.

Twin-roll casting (TRC) 는 금속의 용탕 상태에서 직접 판재로 주조 가능한 연속 주조 공정이다. TRC 공정을 이용하여 원가 절감 및 생산 효율 향상 등 장점을 가지고 있지만 주조 과정에서 형성되는 중심부 편석 및 주조 결함은 최종 판재 품질에 매우 나쁜 영향을 준다. 특히 중심부 편석은 후속 열처리 및 소성가공 공정을 거처도 제거되지 않아 최종 품질에 안 좋은 영향을 끼쳐 편석 형태 및 편석 형성 원인을 규명하는 것은 매우 중요하다고 판단한다.

FEM 전산모사 프로그램인 Deform 을 이용하여 TRC 공정 과정에서 합금의 응고 거동을 분석하였으며 마그네슘 함량 0.5%에서 5.0%까지 변화 시켜 TRC 공정 중에서 온도 분포 및 액상 분율을 산출하였다. TRC 공정 중에서 주조속도의 영향을 조사하였으며 판재 두께 방향 각 지점의 액상 분율 및 변형 거동을 분석하였다.

전산모사 결과를 기반으로 TRC 공정을 이용하여 마그네슘 첨가량 및 공정 변수가 다른 판재를 제조하였다. 실험 결과에 의하면 편석 형태가 공정 변수에 따라 변화하고 낮은 주조 속도에서 Vortex-shape 형태를 가지고 있는 구조가 발견되었으며 이러한 구조는 후속 공정을 거치면

Super fine grain 구조가 발달되어 우수한 기계적 성질을 가진다. 반면에 높은 주조 속도로 제조한 판재에서 Banded 주조 및 Channel 편석이 복합적으로 존재하여 비교적 비균일한 Grain 구조 및 많은 편석 면적이 발견되었다.

또한, 상용 AA6016 합금을 대상으로 최적 공정 변수를 조사하였다. 13 개 공정 변수를 조사한 결과를 기반으로 양산에 도움이 되는 Channel segregation free diagram 을 도식화하였다.